remote sensing

MDPI

Article

Quantitative Analysis of Human Activities and Climatic Change in Grassland Ecosystems in the Qinghai–Tibet Plateau

Chen Ren [1,†], Liusheng Han [1,†], Tanlong Xia [1], Qian Xu [1], Dafu Zhang [1], Guangwei Sun [1] and Zhaohui Feng [2,*]

[1] School of Civil Engineering and Geomatics, Shandong University of Technology, Zibo 255000, China; 23507020858@stumail.sdut.edu.cn (C.R.); hanls@sdut.edu.cn (L.H.); 23507020857@stumail.sdut.edu.cn (T.X.); 24507020872@stumail.sdut.edu.cn (Q.X.); zbzdf@sdut.edu.cn (D.Z.); sun100711@sdut.edu.cn (G.S.)
[2] College of Urban and Environmental Sciences, Peking University, Beijing 100871, China
* Correspondence: fengzh@igsnrr.ac.cn
† These authors contributed equally to this work.

Abstract: Net primary production (NPP) serves as a critical proxy for monitoring changes in the global capacity for vegetation carbon sequestration. The assessment of the factors (i.e., human activities and climate changes) influencing NPP is of great value for the study of terrestrial systems. To investigate the influence of factors on grassland NPP, the ecologically vulnerable Qinghai–Tibet Plateau region was considered an appropriate study area for the period from 2000 to 2020. We innovated the use of the RICI index to quantitatively represent human activities and analyzed the effects of RICI and climatic factors on grassland NPP using the geographical detector. In addition, the future NPP was predicted through the integration of two modeling approaches: The Patch-Generating Land Use Simulation (PLUS) model and the Carnegie–Ames–Stanford Approach (CASA) model. The assessment revealed that the expanded grassland contributed 7.55×10^4 Gg C (Gg = 10^9 g) to the total NPP, whereas the deterioration of grassland resulted in a decline of 1.06×10^5 Gg C. The climatic factor was identified as the dominant factor in grassland restoration, representing 70.85% of the total NPP, as well as the dominant factor in grassland degradation, representing 92.54% of the total NPP. By subdividing the climate change and human activity factors into sub-factors and detecting them with a geographical detector, the results show that climate change and anthropogenic factors have significant ability to explain geographic variation in NPP to a considerable extent, and the effect on NPP is greater when the factors interact. The q-values of the Relative Impact Contribution Index (RICI) and the RICI of the land use change NPP are consistently greater than 0.6, with the RICI of the human management practices NPP and the evapotranspiration remaining at approximately 0.5. The analysis of the interaction between climate and human activity factors reveals an average impact of greater than 0.8. By 2030, the NPP of the natural development scenario, economic development scenario (ED), and ecological protection scenario (EP) show a decreasing trend due to climate change, the dominant factor, causing them to decrease. Human activities play a role in the improvement. The EP indicates a positive expansion in the growth rate of forests, water, and wetlands, while the ED reveals rapid urbanization. It is notable that this is accompanied by a temporary suspension of urban greening.

Keywords: net primary production (NPP); human activities; climatic change; grassland degradation; Qinghai–Tibet Plateau

check for updates

Citation: Ren, C.; Han, L.; Xia, T.; Xu, Q.; Zhang, D.; Sun, G.; Feng, Z. Quantitative Analysis of Human Activities and Climatic Change in Grassland Ecosystems in the Qinghai–Tibet Plateau. *Remote Sens.* **2024**, *16*, 4054. https://doi.org/10.3390/rs16214054

Academic Editors: Michael Sprintsin, Adrián Regos, Lluís Pesquer Mayos, João Gonçalves, João P. Honrado, Salvador Arenas-Castro and Domingo Alcaraz-Segura

Received: 4 September 2024
Revised: 24 October 2024
Accepted: 27 October 2024
Published: 31 October 2024

Copyright: © 2024 by the authors. Licensee MDPI, Basel, Switzerland. This article is an open access article distributed under the terms and conditions of the Creative Commons Attribution (CC BY) license (https://creativecommons.org/licenses/by/4.0/).

1. Introduction

Grassland is amongst the most pervasive vegetation types globally, occupying 20% of the Earth's land area [1]. The ecosystem provides a number of essential services, including regulation of the climate, maintenance of soil and water, and the preservation of biodiversity [2]. Vegetation constitutes a critical component of the global terrestrial ecosystem, facilitating the regulation of the global carbon cycle [3]. In a recent period of time, research

on the topic of grassland vegetation has attracted considerable attention. Net primary productivity (NPP) is defined as the net quantity of carbon regulated by vegetation over a specified period. It is a useful proxy for characterizing vegetation dynamics and assessing the resilience of vegetation to climate change (climate change refers to the change in climate state over a long period of time; it is usually reflected by the statistical differences in climate factors) [4]. NPP is a key determinant of plant growth, organic matter production, and carbon cycling [5] and can be employed to evaluate the status of vegetation growth [6].

NPP can be quantified through direct measurement or through modeling approaches. Nevertheless, these in situ methods are only capable of measuring discrete NPP data over a restricted area, making them unsuitable for estimating NPP at scales exceeding the regional level. With the advent of remote sensing techniques, the generation of high-quality global NPP datasets based on satellite observations and mathematical algorithms has become a viable and reliable approach [7]. The current state of the art in NPP algorithms is sufficiently evolved to support the development of commercial products, thereby providing an excellent data source for the investigation of the regulatory mechanisms of NPP. Nevertheless, it remains challenging to quantify the predominant driving forces that shape grassland ecosystems [8]. Previous investigations have employed the novel climate use efficiency (NCUE) index for the purpose of monitoring grassland restoration and degradation [9] and have constructed a human footprint index that enabled the quantification of the direct and indirect impacts of human activities (human activities refer to a series of activities of different scales and types that human beings have continuously carried out in order to survive and develop and improve living standards, including reclamation, formulation of management policies, etc.) [10], thereby reflecting the comprehensive status of human activities. Alternatively, some of the literature has employed the four-quadrant model of human activities and ecosystem services as a framework for evaluating ecological quality [11]. The literature such as this provides a conceptual framework for understanding the effects of human activities and climatic changes on the eco-systemic environment. Nevertheless, these studies merely quantify the impact of a single category of influencing factors on the ecological environment and are therefore inadequate for capturing the joint impact of climatic factors and human activity factors. In recent years, a substantial body of research has distinguished between the effects of climatic changes and those of human activities. For example, the chemical equations of photochemical reactions are utilized in the Carnegie–Ames–Stanford Approach (CASA) model and Thornthwaite Memorial models to simulate the spatiotemporal characteristics of NPP and its influencing factors [12]. Moreover, the relationship between NPP and the Normalized Difference Vegetation Index (NDVI) is employed to ascertain the quantitative and spatial differentiation of NDVI affected by climatic changes and human activities [8]. Notwithstanding the comprehensive evaluation of the impact of climactic and anthropogenic factors on the ecological environment provided by these studies, the specific consequences of such factors have yet to be quantified. The grazing intensity index [13], night light [14], and urban expansion area [15] are currently the most widely used indices for quantifying human factors. However, the aforementioned studies are insufficient for a thorough assessment of the extent to which human activities are affecting the environment. In order to comprehensively and quantitatively assess the impact of human activities on the environment, Mao put forth the Relative Impact Contribution Index (RICI) [16]. The geographical detector is commonly utilized for the detection of influences exerted by various factors. This quantitative approach enables the discernment of the impact of independent variables on dependent variables [17]. The comprehensive detection of the RICI index and climate factors through the geographical detector can illustrate the interaction between driving factors on vegetation NPP.

The Qinghai–Tibet Plateau is colloquially known to as the "world's third pole", with an average elevation exceeding 4000 m. As the most elevated and extensive plateau on Earth, the Qinghai–Tibet Plateau is distinguished by a unique terrestrial ecosystem. The vegetation on this plateau is particularly vulnerable to climate change [18,19], and the susceptible alpine ecosystem presents a challenge in reconciling the objectives of grassland

conservation and economic advancement [20]. Previous investigations have revealed that the grassland ecosystem is vulnerable to a multitude of factors, including climatic changes and human activities [21,22]. The grass ecosystems in the Qinghai–Tibet Plateau have been significantly degraded by human activities and climatic changes [23]. Since the 21st century, the overall climate trend of the Qinghai–Tibet Plateau has become warmer and wetter (Figure A1) [24], which may contribute to the growth of grassland [25]. However, other studies indicate that the increase in precipitation may have an inhibitory effect on the growth of grassland productivity [26]. In terms of human activities, some research suggests that the primary drivers of grass degradation in the Qinghai–Tibet Plateau are cultivation, animal husbandry, and urbanization [27]. In response to these developments, the Chinese administration has initiated a series of environmental protection initiatives, including the Natural Forest Protection Project, the Three North Shelterbelt Project, etc. [28]. Nevertheless, the impact of these protection policies and climate change on grassland growth remains uncertain [29].

This study focused on the Qinghai–Tibet Plateau as a study area, employing the NPP to investigate the interrelationships between grassland productivity, climatic changes, and human activities [30]. The RICI index was calculated, and the interaction effects of driving factors in the ecologically vulnerable area were assessed by a geographical detector. The estimation of NPP under different future scenarios was accomplished by combining The Patch-Generating Land Use Simulation (PLUS) model and the CASA model [31]. Presently, approximately 30% of the grassland on the Qinghai–Tibet Plateau has been degraded as a consequence of human activities and climate change [32]. Therefore, quantitative investigation of the multiple causal factors of grassland NPP alteration and the resultant effects is of considerable importance for the ecological restoration of the Qinghai–Tibet Plateau [33]. The objective of this study was to investigate the following question: (1) to evaluate the temporal and spatial changes in land use and NPP in the Qinghai–Tibet Plateau over the past two decades, (2) to ascertain the impact of driving factors on grassland growth, and (3) to quantitatively assess the interaction between climatic changes and human activities factors on NPP.

2. Materials and Methods

2.1. Study Area

The Qinghai–Tibet Plateau is situated in the southwestern region of China, between 25°59′N~39°50′N and 73°30′E~104°40′E [34]. The region has a diverse topography and complex environment [35]. The Qinghai–Tibet Plateau extends from the southern margin of the Himalayas in the south to the northern margin of the Kunlun Mountains in the north, the Pamir Plateau in the west, and the Hengduan Mountains in the east (Figure 1). The study area was delineated using boundary vector data for the prefecture-level administrative units located within the Qinghai–Tibet Plateau region. The Qinghai–Tibet Plateau is situated at an altitude of over 4000 m above sea level [36], which gives it a unique plateau climate and a typical monsoon system with low temperature, low humidity, little cloud cover, and abundant sunshine [37]. The mean annually recorded temperature is 1.34 °C and the mean value of the annual precipitation is 323.78 mm. Due to the uneven regional distribution, the temperature at the edge of the plateau is higher than that in the interior. The maximum rainfall area is up to 1000 mm, while the lowest area is only 20 mm. The vegetation communities of the Qinghai–Tibet Plateau are complex and diverse [38]. Most of the vegetation is natural grassland. Grasslands cover an area of about 1,530,000 square kilometers, accounting for nearly 60 percent of the total area of the Qinghai–Tibetan Plateau (https://www.gov.cn/) (accessed on 3 October 2023).

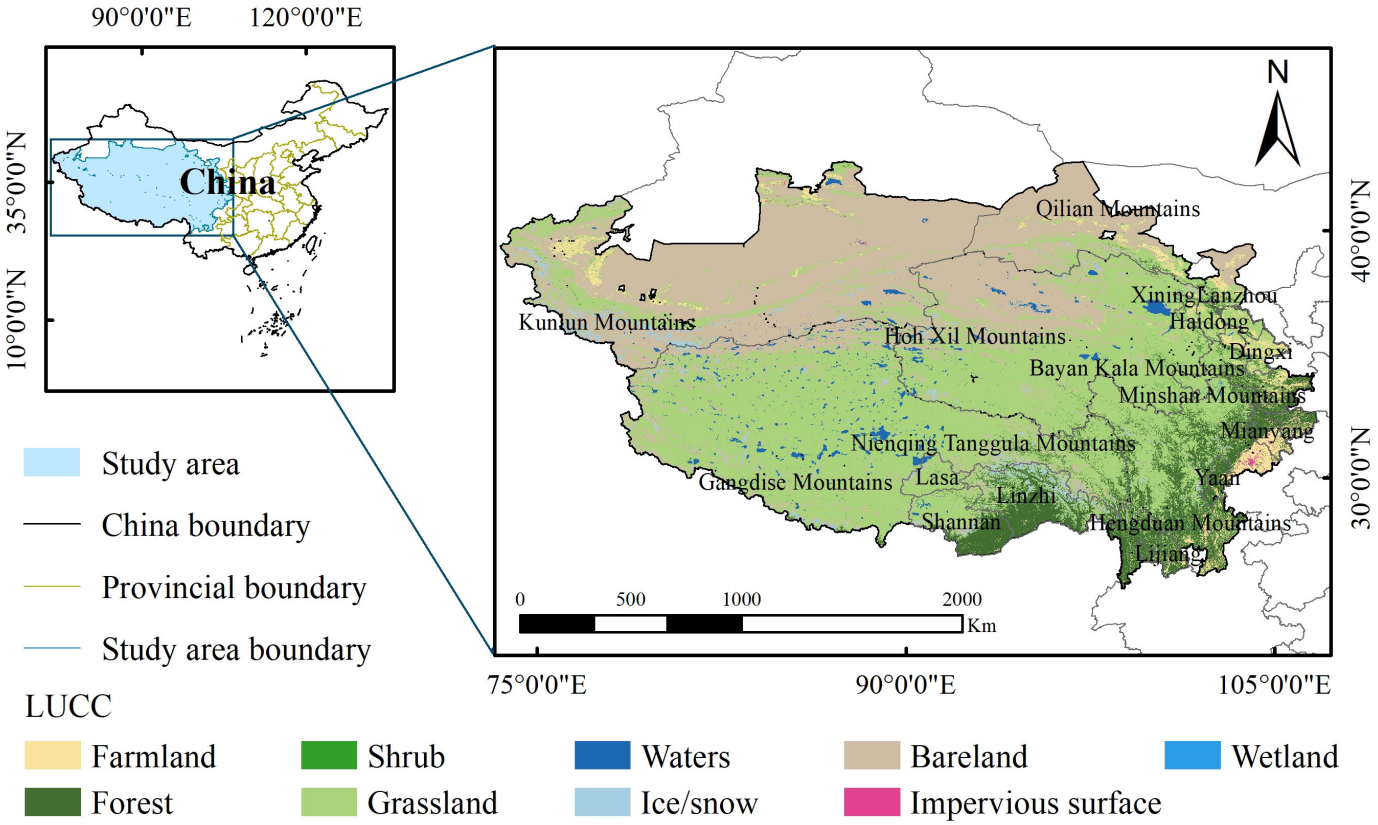

Figure 1. Study area and land use type in 2020.

2.2. Data and Processing

2.2.1. Land Cover Data

The annual China land cover dataset (CLCD) of 2000 and 2020 were obtained from a paper on zenodo (https://zenodo.org/records/8176941) (accessed on 11 February 2023) [39] as Land Use and Cover Change (LUCC) data. These data are based on Google Earth Engine to construct temporal and spatial features, combined with a random forest classifier to obtain classification results. The data coordinate system for CLCD is WGS-84, which has an overall accuracy of 80% and defines a total of nine main categories [39].

2.2.2. Meteorological Data

Historical precipitation (https://data.tpdc.ac.cn/) (accessed on 20 February 2023), temperature, and downward shortwave radiation (https://www.geodata.cn/main/) (accessed on 20 February 2023) were obtained from the National Earth System Science Data Center and the National Tibetan Plateau Science Data Center, respectively. The precision of the data regarding the spatial distribution of temperature and precipitation is 0.0083333°. The future temperature, precipitation (https://data.tpdc.ac.cn/) (accessed on 20 February 2023), and radiation (https://cds.climate.copernicus.eu/) (accessed on 20 February 2023) data are based on the ssp245 medium emission scenario data of CMIP6. Similarly, the resolution of temperature and precipitation data is 0.0083333° and the spatial precision of the radiometric data is 1°, which is generated in China through the Delta spatial downscaling program based on the global 0.5° climate dataset released by CRU and the global high-resolution climate dataset released by WorldClim. The spatial precision of radiation data (SR) is 0.05°, which is based on the inversion of MODIS and AVHRR data, where AVHRR data are estimated using an improved lookup table algorithm and MODIS data are estimated using a hybrid algorithm. Vapor Pressure Deficit (VPD) data came from network sharing, and the spatial resolution was 0.05 degrees.

2.2.3. Other Data

Normalized Difference Vegetation Index (NDVI) (https://www.earthdata.nasa.gov/) (accessed on 22 February 2023) data were obtained from NASA. The NDVI data come from the MOD13A3 dataset regularly released by NASA, and the spatial precision of the data is 1 km. Both Gross Domestic Product (GDP) and population (POP) data were collected from the National Tibetan Plateau Science Data Center. The spatial resolution of GDP and population data is 1 km. These two raster data were spatialized for GDP and the population by integrating multiple factors and assigning weights, which facilitates data sharing and spatial statistical analysis. The data come from the resource and environmental science data registration and publication system, and the linear interpolation of time is performed on the raw data to obtain year-by-year data, which is saved in the GeoTIFF file format. The methodology and standards of the data in previous years are consistent, the coverage is complete, and the collection and processing process is traceable and reliable, (https://doi.org/10.12078/2017121102) (https://doi.org/10.12078/2017121101) (accessed on 22 February 2023). The data pertaining to the road and rail networks were sourced from Baji Data (https://www.bajidata.com/) (accessed on 22 February 2023). These data were in the shape file (SHP) format, and the distance raster data were obtained using the Euclidean distance tool in ArcMap 10.7.

2.3. Methods

In this paper, the RICI index is used as a factor to quantitatively evaluate human activities, and the Geographical detector is used to detect the Single factor and interactive factor effects of RICI with climate factors. Furthermore, it combines the PLUS model and CASA model to predict the NPP under the three scenarios in 2030 for analysis. The technical route is shown in Figure 2. We calculated PNPP to obtain HNPP; combined with the LUCC transfer matrix to obtain MNPP and LNPP; and judged the dominant factor by comparing the size of the absolute value of the slope of PNPP and HNPP. The RICI index, MNPP-RICI, and LNPP-RICI can be calculated from ANPP, PNPP, MNPP, and LNPP and the influence of the RICI index and climate factors on grassland NPP was then detected by using the geographic detector. We obtained the LUCC for the three scenarios in 2030 from the PLUS model and then imported the parameters into the CASA model to calculate the NPP for the three scenarios in 2030.

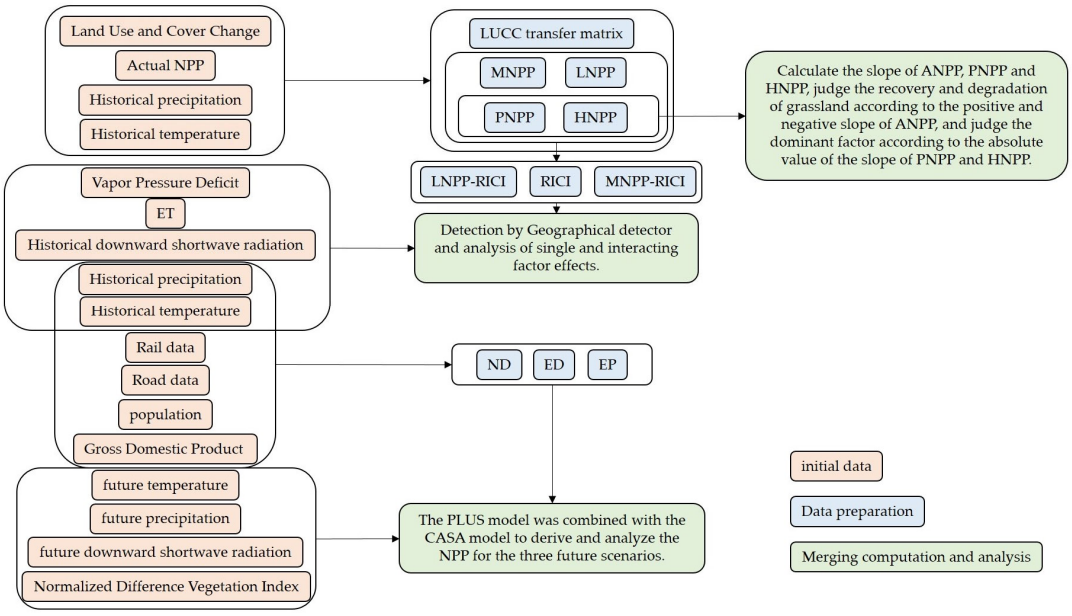

Figure 2. The red boxes represent initial data, the blue boxes represent data to be prepared, and the green boxes merge computation and analysis.

2.3.1. Calculation of NPP and Significance Evaluation

We calculated PNPP and combined with ANPP to obtain HNPP. The land use transfer matrix for each year is calculated and combined with HNPP to obtain LNPP and MNPP and the significance of each NPP is calculated to analyse the trend of NPP changes.

Collection of Actual NPP

The actual NPP (ANPP) was derived from the MOD17A3HGF dataset [40], which had undergone various calibration changes, including modifications to the response-scan angle (RVS) methodology that have an impact on the reflection bands of Aqua and Terra MODIS. Additionally, optical crosstalk in the Terra MODIS infrared band has been rectified, and amendments have been made to updates to the Terra MODIS forward lookup table (LUT) for the period 2012–2017.

Estimation of Potential NPP

The Potential Natural Productivity (PNPP) index may be employed to elucidate the influence of climatic changes on vegetation productivity in grassland ecosystems. PNPP was calculated using the Thornth Waite Memorial model [41,42], which was constructed upon the Miami model. This is expressed as follows:

$$E = 3000 + 25AAT + 0.05AAT^3 \quad (1)$$

$$ET = \frac{1.05ATP}{\sqrt{1 + (1 + 1.05ATP/E)^2}} \quad (2)$$

$$PNPP = 3000\left[1 - e^{-0.0009695(ET-20)}\right] \quad (3)$$

where E is used to denote the annual average evapotranspiration (mm). AAT represents the annually averaged temperature (°C); ET denotes the annual actual total evapotranspiration (mm); ATP signifies the annual total precipitation (mm).

LUCC Change and Corresponding NPP

Combining the LUCC for 2000 with the other years gives the land use transfer matrix for each year, which is then combined with the ANPP data to obtain the area and NPP for each transfer type.

Subdivision of Grassland NPP and Human Activities NPP

It is widely accepted that human activities and climatic changes are the main factors affecting the change in grassland NPP, namely human activities NPP (HNPP) and PNPP, which is the direct cause of the change in the ANPP. The ANPP of grassland for the years 2000 and 2020 is predominantly represented as follows:

$$NPP_{2000} = NPP_{2000\ unchange} + NPP_{out} \quad (4)$$

$$NPP_{2020} = NPP_{2020\ unchange} + NPP_{in} \quad (5)$$

where NPP_{2000} is the ANPP of grassland in 2000; NPP_{2020} specifies the ANPP of grassland in 2020; and "2000unchange" represents the grassland area that did not change in 2000 in the transfer from 2000 to 2020, which means that it is a grassland area in both 2000 and 2020. "2000unchange" and "2020unchange" represent the same regional extent. NPP2000unchange and NPP2020unchange are obtained by mask extraction of the NPP in the corresponding regions; "in" and "out" are relative to grassland, with "in" referring to areas where other land-use types have converted to grassland; and "out" refers to areas where grassland has been converted to other land-use types. Mask extraction of the ANPP based on the extent of the "in" and "out" regions yields NPP_{in} and NPP_{out}.

HNPP can be subdivided into NPP caused by land use change (LNPP) and NPP caused by human management practices (MNPP). The area of grassland converted to grassland (grassland unchanged) is the management measure in human activities, while the area of mutual transfer between grassland and other land use types is the land use change in human activities. By computing HNPP on the corresponding regions, MNPP and LNPP can be obtained. The calculation of LNPP and MNPP can be derived from the expression of ANPP and PNPP, as follows:

$$LNPP_{2020} = NPP_{in} - NPP_{climate-change} \quad (6)$$

$$LNPP_{2000} = NPP_{out} - NPP_{climate-change} \quad (7)$$

$$MNPP_{2020} = NPP_{2020\ unchange} - NPP_{climate-unchange} \quad (8)$$

$$MNPP_{2000} = NPP_{2000\ unchange} - NPP_{climate-unchange} \quad (9)$$

where $NPP_{climate\text{-}change}$ is PNPP in the context of incremental grassland. $NPP_{2020unchange}$ represents the NPP of 2020 constant grassland; the $NPP_{2000unchange}$ indicator refers to the NPP of a steady grassland ecosystem in the year 2000; and the $NPP_{climate\text{-}unchange}$ represents the PNPP of the grassland area that has remained unaltered [41].

Dynamic Analysis of Grassland Ecosystems

This research focused diverse types of NPP for the purpose of evaluating grassland productivity and its underlying drivers. To analyze the changes in grass NPP, we applied the least squares regression. To ascertain the significance of the observed variation, we employed an approach that involved calculating a slope and utilizing the associated F-test to ascertain the confidence interval [41]. The following formula is to be employed:

$$slope = \frac{n \times \sum_{i=1}^{n} (i \times NPP_i) - \sum_{i=1}^{n} i \sum_{i=1}^{n} NPP_i}{n \times \sum_{i=1}^{n} i^2 - (\sum_{i=1}^{n} i)^2} \quad (10)$$

$$F = (n - 2) \times \frac{U}{Q} \quad (11)$$

$$U = \sum_{i=1}^{n} \left(\hat{y}_i - \bar{y}\right)^2 \quad (12)$$

$$Q = \sum_{i=1}^{n} (y_i - \hat{y}_i)^2 \quad (13)$$

where i represents a number between 1 and 21, with 1 representing the year 2000 and 21 representing the year 2021. The variable n is set to 21, corresponding to the study period. As indicated by NPP_i, the value of NPP in year i can be determined. U represents the summation of squares pertaining to regression, whereas Q represents the summation of squares pertaining to error; yi refers the actual NPP in the i year. The regression value, represented by the letter $\hat{y}_i$ signifies the average NPP over the 21-year period, which is indicated by the letter $\bar{y}$. The F-test is a statistical tool that can be used to ascertain the significance of a modification in the NPP.

2.3.2. Assessment of the Dominant Factor

Using the ANPP, PNPP, and HNPP calculated in the previous sections, grassland restoration and degradation were judged by the positive and negative relationship of ANPP, and the dominant driver was judged by the relationship between the absolute magnitude of the slopes of PNPP and HNPP.

The distinction between grass growth and degradation may be discerned through an examination of the slope of ANPP (AS), as calculated by using Equation (10). The different scenarios are shown in Table 1. The comparison of absolute slope values of PNPP (CS) and HNPP (HS) can assess the impact of driving factors. When AS is greater than 0 and |CS| is greater than |HS|, the climate factor is considered to be the main driver of the increase in

AS. When AS is greater than 0 and |CS| is less than |HS|, human activities are considered to be the main driver of the increase in AS. When AS is less than 0 and |CS| is greater than |HS|, the climate factor is considered to be the main driver of the reduction in AS. When AS is less than 0 and |CS| is less than |HS|, human activities represent the preponderant causal factor of AS reduction [43].

Table 1. Scenarios to ascertain the influence of driving factors on the condition of grassland ecosystems. (AS, CS, and HS represent the trend slope of change for ANPP, PNPP, and HNPP in each pixel).

Grassland Condition	Method (Slope Comparison)	Roles of Factors About Climate and Human Activities
Restoration (AS > 0)	|CS| > |HS|	Climate-caused (CDR)
	|CS| < |HS|	Human activities-caused (HDR)
Degradation (AS < 0)	|CS| > |HS|	Climate-caused (CDD)
	|CS| < |HS|	Human activities-caused (HDD)

2.3.3. Detection of Single and Interacting Factors

The RICI index, ATP, AAT, radiation, ET, and VPD were probed using a Geographical detector to obtain the single and interactive factor effects for each factor.

Relative Impact Contribution Index (RICI)

Extensive studies have been conducted based on PNPP and ANPP to quantitatively determine how climatic changes and human activities affect vegetation NPP [44]. The RICI has been established as a quantitative index for evaluating the effect of human activities on grassland NPP. The calculation is as follows:

$$\mathrm{RICI} = \frac{\mathrm{PNPP} - \mathrm{ANPP}}{\mathrm{PNPP}} \tag{14}$$

An RICI value greater than zero implies that human activities are having a deleterious impact on NPP. Conversely, a negative RICI value indicates that human activities are beneficial for the maintenance of grassland NPP. It can be seen that there is a direct correlation between the magnitude of the RICI and the degree of impact that human activities have on the alteration of grassland NPP [16].

Geographical Detector

The geographical detector represents a statistical method of detecting spatial heterogeneity and of elucidating the factors influencing this phenomenon. Through the quantitative analysis of the total discrepancy between the different types of geographic space, the Geographical Detector is capable of determining the extent to which the independent variables exert influence on the dependent variables [45]. The present study makes use of both the single-factor and the interaction detectors in order to ascertain the impact of climate change factors and human activity factors in NPP. In single-factor detection and interactive detection, the influence of factors is evaluated by the q value. Previous studies have found that when the condition of $p < 0.01$ was satisfied, the p and q values of the factors were considered to be statistically significant [46].

Single-factor detection primarily identifies the extent to which an independent variable influences the spatial heterogeneity of a dependent variable. This is achieved by utilizing the value of q to assess the influence degree of the independent variable, thereby facilitating the detection of factors that impact the spatial heterogeneity of the dependent variable. The first step is to detect the spatiotemporal variation in variable Y. The following step is to ascertain the influence of factor X on this variability. The test result is represented by q value [46], as follows:

$$\mathrm{q} = 1 - \frac{\mathrm{SSW}}{\mathrm{SST}} \tag{15}$$

$$SSW = \sum_{h=1}^{L} N_h \sigma_h{}^2 \quad (16)$$

$$SST = N\sigma^2 \quad (17)$$

where q represents the influence of factors on NPP, that is, the strength of explanatory power. h = 1, . . . L; and L refers to the stratification of either variable Y or factor X. N_h and N denote the number of sampled units in the differentiated area and the entire area, respectively. The variances of RSEI in differentiated areas and the entire area are represented by $\sigma_h{}^2$ and σ^2, respectively. SSW is used to describe the overall variance of differing layers, whereas SST represents the region-specific summation of this variance. The value range of q is defined as [0, 1]. The greater the proximity of q to the value of 1, the more pronounced the effect of the influencing factor on the NPP [17].

The interaction detector is employed to identify the interaction of disparate influencing factors on the dependent variable. Subsequent to the interaction detection of the aforementioned influencing factors, there are typically five cases: nonlinear weakening, single-factor nonlinear weakening, two-factor enhancement, nonlinear strengthening, and mutual independence [47]. In this study, the mesh size of each fishing net was 0.1 degrees square.

2.3.4. NPP Prediction

The prediction of NPP comprises four principal steps. The initial step is to utilize the PLUS model to forecast the LUCC under three distinct development scenarios. The second step is to employ the CASA model to calculate the 2020 NPP for verification purposes. The third stage of the process entails utilizing multiple linear regression to predict the NDVI in 2030. The subsequent step is the utilization of the CASA model for the purpose of forecasting future NPP.

Patch-Generating Land Use Simulation (PLUS) Model

The PLUS model is a cellular automaton (CA) model founded upon raster data, which is capable of simulating LUCC alterations. The proposed model demonstrated superior simulation accuracy and exhibited landscape pattern metrics that were more closely aligned with the true landscape than those observed in other CA models under investigation [48]. This paper selects six driving factors from three aspects: ATP, AAT, GDP, POP, and distance from highway and distance from railway. The first step is to employ a Markov model to forecast prospective land use data for a natural development scenario (ND). Subsequently, a conversion probability matrix is modified under two alternative scenarios, namely an economic development scenario (ED) and an ecological protection scenario (EP). Finally, the future land use data for the aforementioned scenarios are predicted. In this paper, the Kappa statistic is employed to assess the precision of the simulation outcomes. The Kappa statistic ranges from 0 to 1, with values exceeding 0.7 denoting a substantial degree of consistency and accuracy in the simulation results [49,50]. The formula is presented below, as follows:

$$Kappa = \frac{P_0 - P_1}{P_2 - P_1} \quad (18)$$

where P_0 represents the correct proportions of the simulation, P_1 represents the correct proportions of the model in the random case, and P_2 represents the correct proportions of the simulation in the ideal classification case [51]. Verification of the model revealed a kappa statistic of 0.8928, indicating a high level of accuracy in the simulation. The model demonstrated the capacity to accurately reflect the LUCC in the Qinghai–Tibet Plateau, a capability that can inform future forecasts for the year 2030.

Estimation and Verification of NPP

In this study, the CASA model is employed for estimating net primary production (NPP), whereby NPP is determined by multiplying the absorbed photochemical active radiation (APAR) in green vegetative matter by the light energy utilization efficiency (ε) and NPP is determined by employing the following formula:

$$NPP(x, t) = \varepsilon(x, t) \times APAR(x, t) \quad (19)$$

$$\varepsilon(x, t) = T_{\varepsilon 1}(x, t) \times T_{\varepsilon 2}(x, t) \times W_{\varepsilon}(x, t) \times \varepsilon_{max} \quad (20)$$

$$APAR(x, t) = SOL(x, t) \times FPAR(x, t) \times 0.5 \quad (21)$$

the variable x represents a pixel, while t represents time; ε(x, t) represents the quantity of light energy absorbed by pixel x during the month indicated by the subscript, with the unit of measurement is g C·MJ-1; and APAR(x, t) represents the radiation produced by pixel x in month t when the pixel is engaged in photosynthetic activity. The unit of measurement for this radiation is g C/(m^2·month); $T_{\varepsilon 1}(x, t)$ represents the limiting effect of vegetation at low and high temperatures, while $T_{\varepsilon 2}(x, t)$ denotes the ambient temperature to which the vegetation is exposed; $W_{\varepsilon}(x, t)$ signifies the effect of humidity conditions on the use of light energy; ε_{max} is the maximum light energy utilization under ideal conditions; $SOL(x, t)$ represents the total solar radiation at pixel x in month t; $FPAR(x, t)$ is the proportion of incident photosynthetically active radiation absorbed by the vegetation layer; and the constant 0.5 represents the fraction of solar radiation that can be used by vegetation as effective solar radiation [52].

The estimated NPP and actual NPP were verified by taking uniform points. First, the 2020 NPP was estimated by the CASA model, then fishing nets were constructed, and the estimated NPP and actual NPP were sampled according to different land use types, with a total of 2357 data points.

The prediction method used in this paper requires fewer parameters for NPP prediction. It allows for the prediction of NPP values using both past and future data and taking into account landuse change, resulting in more accurate and reasonable predictions. Future vegetation type data, which can be predicted by the PLUS model (a land-use prediction model), are necessary to predict NPP using the CASA model. The PLUS model achieves better simulation accuracy compared with the CA-Markov model and the FLUS model for land use prediction [31].

3. Results and Discussion

3.1. LUCC Change and Corresponding NPP in the Qinghai–Tibet Plateau

The LUCC exerts an immediate impact on plant productivity as a consequence of human activities [53,54]. As illustrated in Figures 3a and 4a, the conversion of bareland into grassland (6.45%) is predominantly concentrated in the Qilian Mountains in the northeast, the cross-zone between bareland and grassland in the southwest Qinghai–Tibet Plateau. Similarly, the conversion of farmland to grassland (11.77%) is primarily concentrated in the eastern Dingxi City, Lanzhou City, and the Qilian Mountains, as well as the western Kashgar area. This transformation in land utilization has been made feasible as a consequence of the introduction of ecological conservation policies, including the conservation of natural forests [55,56]. The transformation of farmland into forest and grassland [57] and the creation of protected areas designated for the preservation of natural habitats [58,59]. Whereas, the degradation of grassland on the Qinghai–Tibet Plateau is predominantly concentrated in northern Tibet and northwestern Qinghai (Figure 3b). The alteration from grassland to bareland, woodland, and farmland is clearly discernible [60–62]. The alteration of grassland to bareland (3.87%) was primarily concentrated in the western Kunlun Mountains. The transformation of grassland into farmland (0.92%) was primarily situated in the eastern Minshan Mountains and the western Kashgar region (Figures 3b and 4a). Furthermore, the conversion of grassland to forest land (0.7%) was predominantly concen-

trated in eastern Longnan City and the southeastern Garze Tibetan Autonomous Prefecture (Figures 3b and 4a). The loss of vegetation cover may be attributed to overgrazing [37]. The findings indicated that grassland degradation was more pronounced than restoration on the Qinghai–Tibet Plateau, exhibiting a downward trajectory. The application of ecological conservation measures has been demonstrated to exert a significant beneficial effect on the restoration and sustainable development of grassland and forest on the Qinghai–Tibet Plateau to a certain extent [63]. However, the impact of these policies may be outweighed by the combined effects of overgrazing, climatic changes, and unfavorable environmental conditions [55].

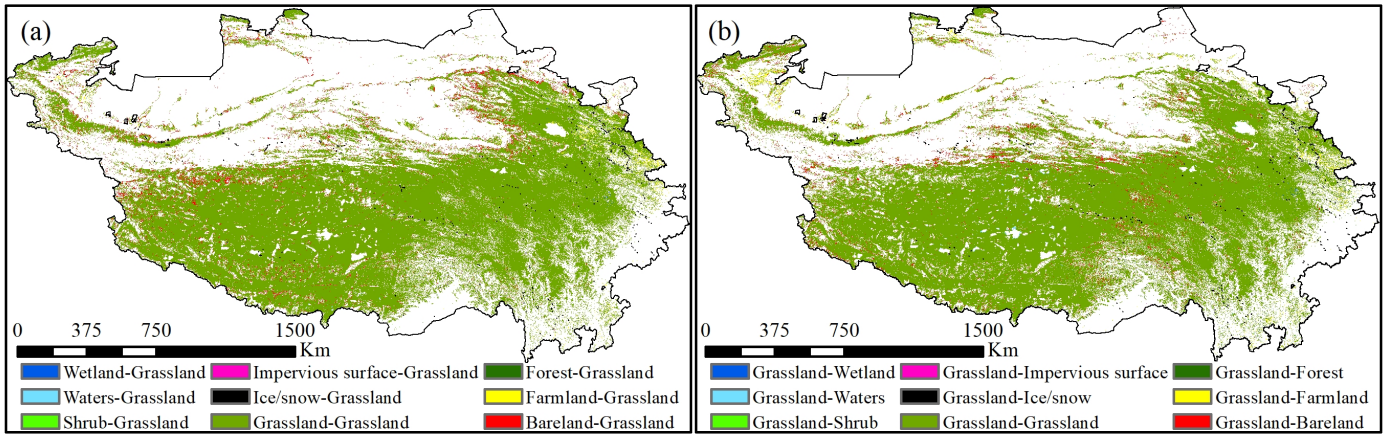

Figure 3. Geographical distribution characteristics of grassland and other LUCC on the Qinghai–Tibet Plateau from 2000 to 2020. Figure (**a**) depicts the conversion of the Qinghai–Tibet Plateau from LUCC to grassland. Figure (**b**) illustrates the transformation of grassland into other LUCC within the same region.

The extent of grassland that has transformed into other land uses, as well as the area of other land uses that have been transformed into grassland, was 6.99×10^4 km^2 and 6.71×10^4 km^2, respectively (Table A1). By the year 2020, the mean NPP loss was predominantly attributed to the conversion of grassland to forest (456.36 C/(m^2·yr)) and shrub (418.05 g C/(m^2·yr)). While the increase was mainly the transfer of forest (425.39 C/(m^2·yr)) and shrub (379.04 C/(m^2·yr)) to grassland (Figure 4b). The total NPP loss in grassland was 1.06×10^5 Gg C. The predominant cause of this decline can be attributed to the conversion of grassland to farmland and forest, which accounts for 3.58×10^4 Gg C and 4.11×10^4 Gg C (Figure 4c). The total NPP from the expansion of grassland in 2020 was 7.55×10^4 Gg C, of the total NPP derived from farmland was 4.13×10^4 Gg C, followed by bareland, 1.96×10^4 Gg C (Table A1). It can be observed that the MNPP and PNPP are 3.46×10^4 Gg C and -1.89×10^4 Gg C, respectively (Figure A2), in comparison to the total NPP estimated for unmanaged grassland in 2000. The total NPP increase attributed to land use change was 5.49×10^3 Gg C, with an additional 7.57×10^3 Gg C transferred from grassland (Figure A2). In general, the total NPP driven by human activities demonstrated an upward trajectory during the period between 2000 and 2020 [64]. Conversely, the NPP driven by climate change presented a declining trend. It has been demonstrated that human activities can positively influence the expansion of grassland NPP and that human activity can also play a role in mitigating grassland degradation by regulating climate [65].

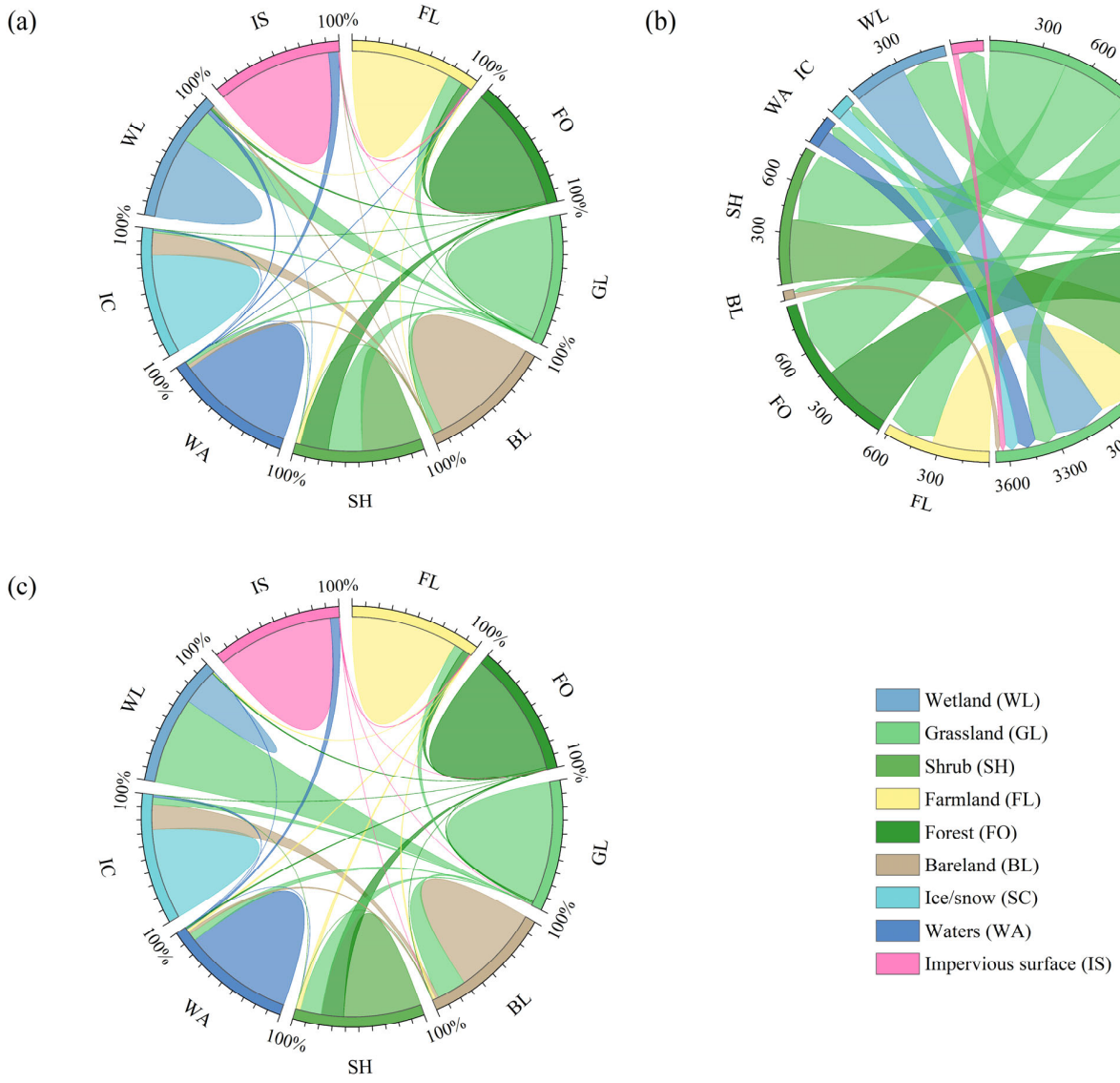

Figure 4. Chord diagrams of LUCC change area (**a**), mean (**b**) and total (**c**) NPP.

3.2. Spatial Distribution and Significance Analysis of Different NPP

The ANPP is greater than 200 g C/(m^2·yr) in the southeast regions, while the northwest regions are between 0~200 g C/(m^2·yr) [66]. For PNPP, the southeast regions are greater than 450 g C/(m^2·yr), while the northwest regions are between 0 and 450 g C/(m^2·yr). The spatial distribution of MNPP and LNPP is the opposite, the southeast is lower than −500 g C/(m^2·yr), and the northwest is higher than −500 g C/(m^2·yr) (Figure 5a,b,d,e,g,h,j,k). It is noteworthy that the PNPP is considerably larger than the ANPP (Figure 5a–e). PNPP is larger than 350 g C/(m^2·yr) in most areas, while ANPP is smaller than this value in most areas. A significant increase ($0.01 < p \leq 0.05$) and an extremely significant increase ($p \leq 0.01$) in ANPP were observed to be predominantly localized in the northeast and central regions of the Qinghai–Tibet Plateau, encompassing the northern Tibet Plateau and the Qilian Mountains (Figure 5c). The increase in NPP may be attributed to an increase in humidity [66,67]. In contrast, the ANPP in the Nienqing Tanggula Mountains and the southwestern Tibet Autonomous Region demonstrated a declining trend (Figure 5c), which is in accordance with the results of a previous study [68]. The significant and extremely significant decreases in ANPP were localized in the Lhasa and Nyingchi City areas (Figure 5c). These decreases may be attributed to the low temperatures observed in these regions [69]. The significant increase in PNPP was primarily concentrated in the eastern portion of the Qinghai–Tibet

Plateau, whereas the significant decrease in PNPP was distributed across the southeastern regions of Nyingchi City and Lhasa City (Figure 5f). The LNPP exhibited an upward trajectory in the southeastern and western regions of the Qinghai–Tibet Plateau (Figure 5i). The significance of MNPP is consistent with that of LNPP but opposite that of PNPP. There was a notable increase in a few areas in the central and western regions (Figure 5l).

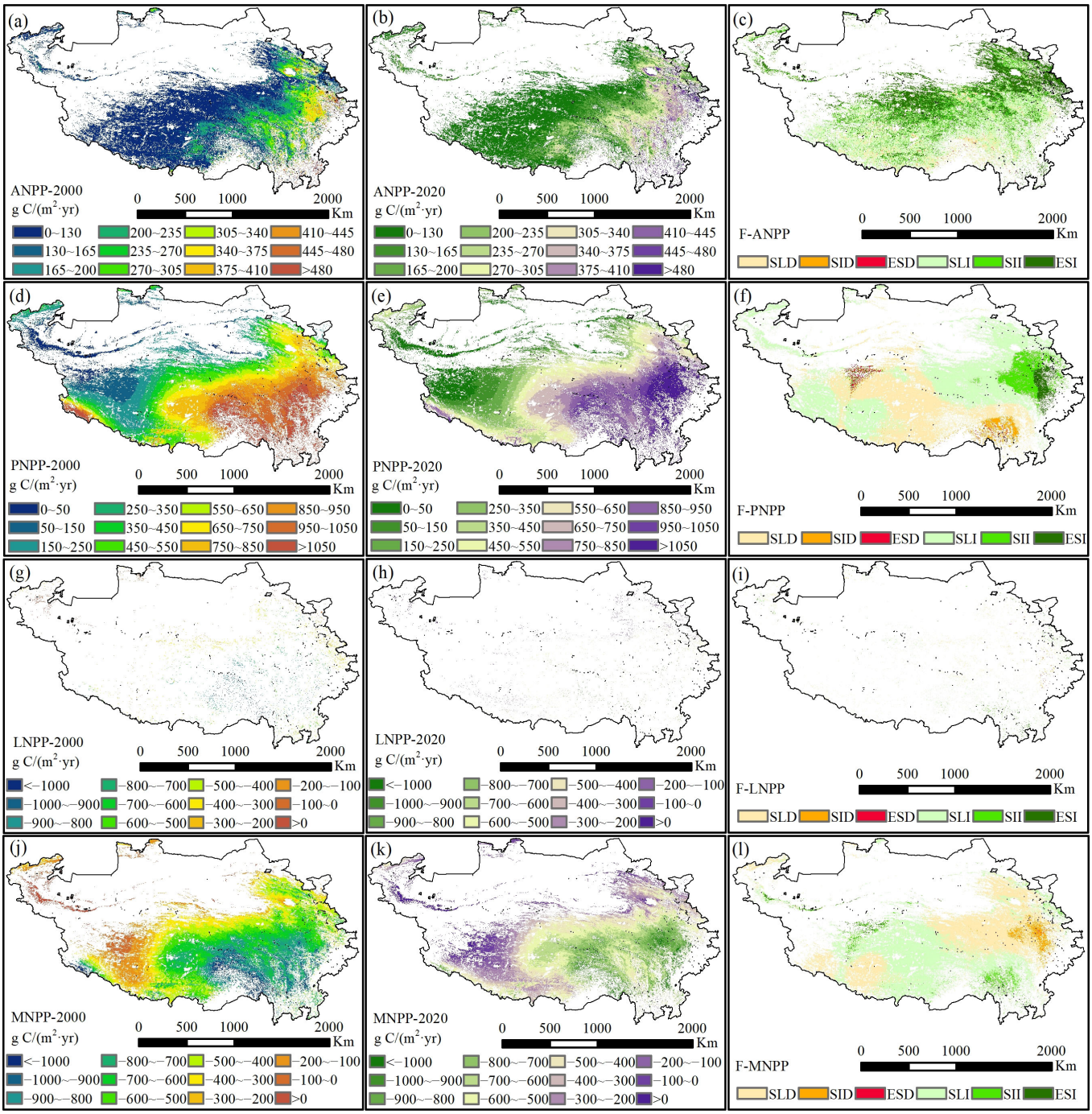

Figure 5. The geographical distribution of ANPP, PNPP, LNPP, and MNPP in the Qinghai–Tibet Plateau in 2000 (**a**,**d**,**g**,**j**) and 2020 (**b**,**e**,**h**,**k**) and the corresponding significance analysis during 21 years (**c**,**f**,**i**,**l**). Decreased cases are a slight decrease (SLD), significant decrease (SID), and extremely significant decrease (ESD). Increased cases are a slight increase (SLI), significant increase (SII), and extremely significant increase (ESI).

3.3. The Impact of Driving Factors on the Change in NPP

The transformation of ecosystems influenced by a complex interplay of factors, the dominant influence of which can be attributed to climatic changes and human activities [70]. The majority of grasslands on the Qinghai–Tibet Plateau exhibited indications of restoration (Figure 6a). Restoration areas that are characterized by human activities are predominantly located in the northern Tibetan Plateau of the Qinghai–Tibet Plateau, the Brahmaputra River basin, and the Lancang River basin (Figure 6a). This is largely attributable to the regulation and intervention in grazing capacity [71]. The climate-dominated restoration areas are predominantly located in the vicinity of rivers and lakes in the eastern portion of the Qinghai–Tibet Plateau (Figure 6a). The areas exhibiting signs of degradation are primarily concentrated in the southeastern regions of the Qinghai–Tibet Plateau (Figure 6b). The areas exhibiting degradation are predominantly situated in the southern areas of the Tibetan Autonomous Region, as well as in the Bayan Kala Mountains (Figure 6b). These areas have been degraded primarily as a result of human activities. This distribution may be associated with the engineering of the Qinghai–Tibet Trans-Himalayan railway, as well as the influx of local residents and tourists [72]. The climate-dominated degraded areas are primarily situated in the southeastern region of the Qinghai–Tibet Plateau, encompassing the southern Tibetan valley and the Nianqing Tanggula mountain range (Figure 6b). These areas experience relatively high temperatures, which may impede vegetation growth [73]. Furthermore, the distribution of degraded grassland is markedly less extensive than that of restored grassland [69].

It was determined that human activities and climatic changes were responsible for 43.11% and 56.89% of the recovery of grasslands in the Qinghai–Tibet Plateau, respectively, with climate change considered the primary factor (Figure 6c). With respect to grassland degradation in the Qinghai–Tibet Plateau, human activities and climatic changes were identified as contributing 29.77% and 70.23%, respectively. Similarly, climatic changes were identified as the predominant factor (Figure 6c). The extent of grassland degradation attributable to climatic changes is greater than that attributable to human activities (Figure 6c). These findings are consistent with those of a previous study [74]. It is commonly acknowledged that the growth of vegetation is most significantly influenced by the availability of water. Therefore, a shortage of water may be a principal factor in the process of grassland degradation [75]. It was demonstrated that the regrowth of grassland resulted in an enhancement in NPP, whereas a diminution in NPP as a consequence of grassland degradation was observed [76]. From 2000 to 2020, the NPP reduction resulting from grassland degradation in the Qinghai–Tibet Plateau was −627.35 Gg C. Climatic change was identified as the dominant factor, accounting for 92.54% (Figure 6d). With respect to the alteration in NPP resulting from grassland restoration, climate change persists as the predominant factor, with an increase of 1127.14 Gg C, representing a proportion of 70.85% (Figure 6d).

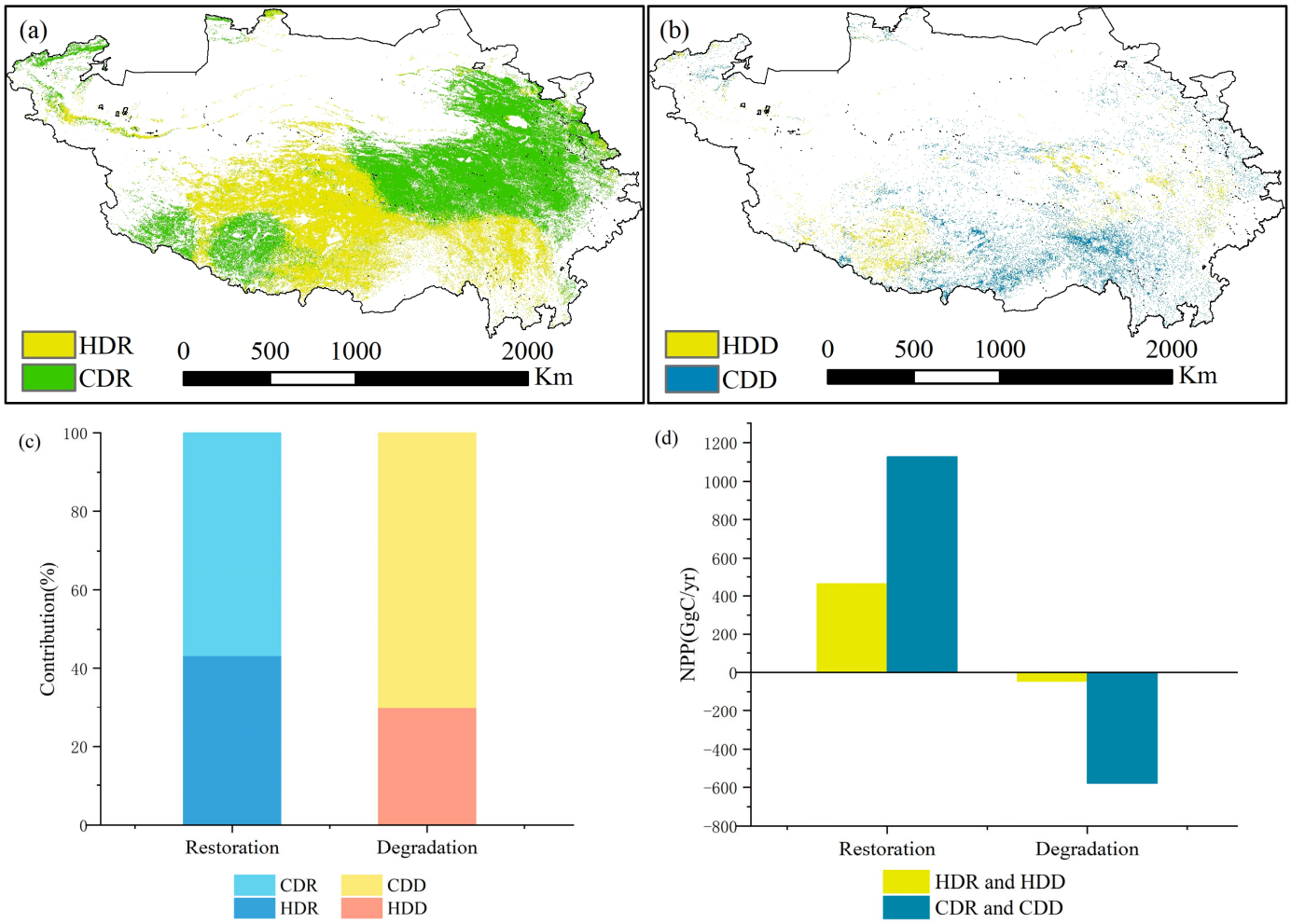

Figure 6. The geographical distribution of grassland degradation in Qinghai–Tibet Plateau (**a**) and restoration in Qinghai–Tibet Plateau (**b**) induced by climatic changes and human activities. Contribution of driving factors to grassland health contribution (**c**). The analysis of grassland NPP due to its contribution to the health of different driving factors (**d**). HDD, CDD, HDR, and CDR represent human-dominated degradation, climate-dominated degradation, human-dominated restoration, and climate-dominated restoration, respectively.

3.4. Detection and Analysis of Climate Change Factor and Human Activity Factor of NPP

3.4.1. Analysis of the RICI Index

The LNPP-RICI represents the RICI of the calculated NPP of land use transfer, while the MNPP-RICI denotes the RICI of the calculated NPP of management measures. It can be seen that the RICI in the northwestern region of the North Tibet Plateau showed negative values (Figure 7a,b) and the growth of grassland NPP is caused by human activities to a certain extent [71]. The RICI value in other areas is predominantly positive, indicating that human activities have contributed to a decrease in grassland NPP (Figure 7a,b) [72]. The RICI value in the western part of the Tibet Autonomous Region, in the vicinity of Xining City and Lhasa City, is predominantly situated between 0 and 0.4 (Figure 7a), indicating a relatively minimal influence of human activities. It is evident that policy management can exert a considerable influence on the Earth's environment. Furthermore, human activities have been demonstrated to facilitate grassland restoration [77]. In order to safeguard the Qinghai–Tibet Plateau's grassland resources, China has established some comprehensive environmental protection policies, aiming to achieve a harmonious balance between economic advancement and environmental stewardship [78]. In Xinjiang, Tibet, Qinghai, and other pastoral regions, grassland restoration has been advanced through

techniques such as fencing, replanting, and plowing [79]. The RICI of the northern Tibetan Plateau, the south of the Gangdise Mountains, the Nianqing Tanggula Mountains, and the Bayan kala Mountains are scattered between 0.6 and 1 (Figure 7a). It can be observed that human activities exert a considerable influence on these regions, with the influence of human activities being greater than that of climate conditions. The Northern Tibetan Plateau has the widest distribution of lakes in China [80] and is one of the most important grazing ecosystems in the world [81]. In pastoral areas, alterations in livestock distribution resulting from shifts in pasture property rights may intensify the pressure on certain pastures, leading to human activities such as overgrazing due to an imbalance in resource systems. This, in turn, may have a detrimental impact on grassland ecosystems [82]. The majority of nomadic activities are concentrated in the foothills and intermountain valleys [83,84], which is why the index is high in the vicinity of the Gangdises, Niench Tanggula, and Bayan Kala mountains (Figure 7a). The LNPP-RICI spatial distribution is generally consistent with the MNPP-RICI spatial distribution. Situated in the southern region of the Qinghai–Tibet Plateau (Figure 7b), the expansion of urban areas has resulted in a significant reduction in the extent of natural habitats, leading to a decline in grassland NPP [85]. The Sanjiangyuan area, which is of great ecological fragility, will be significantly impacted by human activities [86].

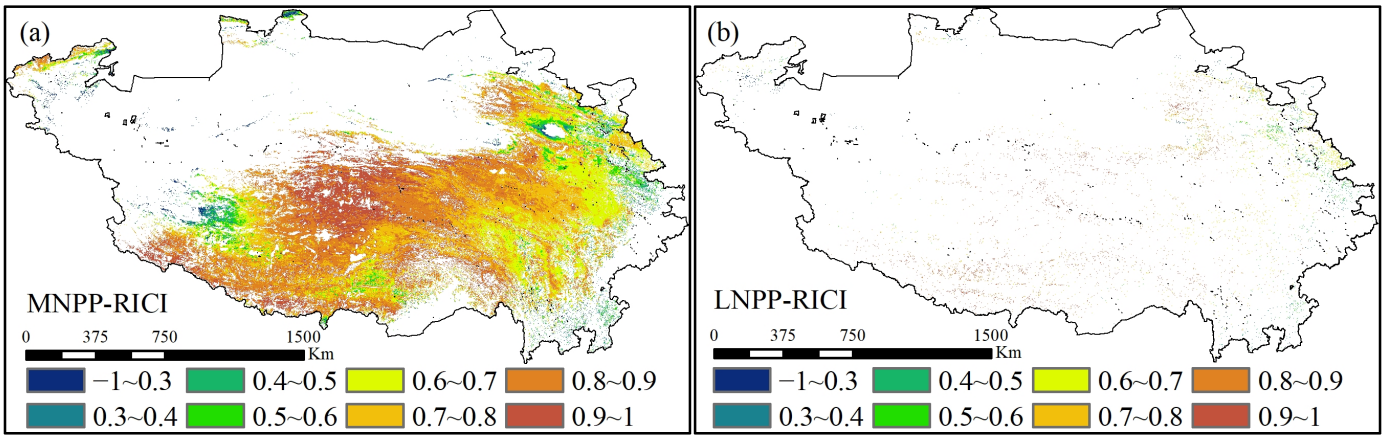

Figure 7. Spatial pattern of relative impact contribution rate index of human activities. The picture (**a**) is the RICI index of constant grassland, and the picture (**b**) is the RICI index of land use transformation.

3.4.2. Analysis of the Single-Factor Detector

The *p*-values of the selected factors are all equal to zero (Table 2), which indicates that the variables exert a significant impact on the spatial heterogeneity of NPP. This result also corroborates the assertion that temperature, precipitation, evapotranspiration, VPD, and radiation are the most significant factors influencing grassland phenology, as documented in the literature [87–91]. The q-values of ET, ATP, and RICI are particularly noteworthy (Table 2). In alpine ecosystems such as the Qinghai–Tibet Plateau, vegetation NPP, is significantly influenced by precipitation and ET changes [92,93]. Compared to MNPP-RICI and LNPP-RICI displays a higher q value (Table 2), indicating that land use is a primary means through which humans impact the ecosystem [94,95], while the climate factor is still the dominant factor in the whole region.

Table 2. q value and *p* value of each influencing factor.

Influence Factor	2000 *p* Value	2000 q Value	2010 *p* Value	2010 q Value	2020 *p* Value	2020 q Value
ET	0.000	0.696	0.000	0.670	0.000	0.674
ATP	0.000	0.676	0.000	0.669	0.000	0.683
RICI	0.000	0.714	0.000	0.670	0.000	0.626
VPD	0.000	0.250	0.000	0.426	0.000	0.321
AAT	0.000	0.623	0.000	0.604	0.000	0.630
SR	0.000	0.610	0.000	0.562	0.000	0.493
ET	0.000	0.569	0.000	0.480	0.000	0.564
ATP	0.000	0.568	0.000	0.479	0.000	0.543
LNPP-RICI	0.000	0.746	0.000	0.695	0.000	0.683
VPD	0.000	0.324	0.000	0.256	0.000	0.352
AAT	0.000	0.476	0.000	0.354	0.000	0.519
SR	0.000	0.515	0.000	0.401	0.000	0.555
ET	0.000	0.442	0.000	0.496	0.000	0.472
ATP	0.000	0.426	0.000	0.484	0.000	0.486
MNPP-RICI	0.000	0.519	0.000	0.549	0.000	0.456
VPD	0.000	0.085	0.000	0.235	0.000	0.069
AAT	0.000	0.246	0.000	0.222	0.000	0.315
SR	0.000	0.505	0.000	0.469	0.000	0.444

3.4.3. Analysis of the Interaction Detector

The interaction detection outcomes illustrate that the combined q-value of all influencing factors following interaction is greater than the individual q-values of each factor within the interaction, indicating a two-factor enhancement (Figure 8). The q value of RICI's interaction with ET and ATP is consistently the highest among the three modules. Furthermore, in the MNPP-RICI module, both ET and MNPP-RICI, as well as ATP and MNPP-RICI, demonstrate nonlinear enhancement (Figure 8). The impact of varying levels of grazing on the spatial heterogeneity of the entire plateau grassland ecosystem was found to be significant [71]. In the Qinghai–Tibet Plateau, precipitation exerts a profound influence on vegetation growth [96]. The decisive factors of ET are precipitation and temperature [88], which explains the significant interaction effect of ET and ATP with RICI and the nonlinear enhancement in the MNPP-RICI module. In the LNPP-RICI module, ET, AAT, ATP, and AAT demonstrate nonlinear enhancement (Figure 8). ET is notably correlated with temperature, and an increase in temperature will exacerbate evapotranspiration [97,98]. Temperature and precipitation are due to the fact that the synchronization of rain and heat will promote the accumulation of NPP [99]. In three modules, the influence of the anthropogenic factors increased greatly after interacting with the climate factors, indicating that human activities also affect grassland NPP by influencing climate [100].

3.5. NPP Prediction of Qinghai–Tibet Plateau Under Multiple Scenarios

3.5.1. Accuracy Verification of NPP Estimation

The average NPP simulated and actual values of 2307 verification points are 309.73 g C/(m^2·yr) and 265.20 g C/(m^2·yr), respectively (Figure 9). There is a statistically significant positive linear relationship between the simulated value of NPP and the actual value, with a correlation coefficient of 0.752 and an average relative error of 16.79% [52], which indicates that the overall simulation effectiveness of the CASA is relatively good. The data points are situated close to the 1:1 line.

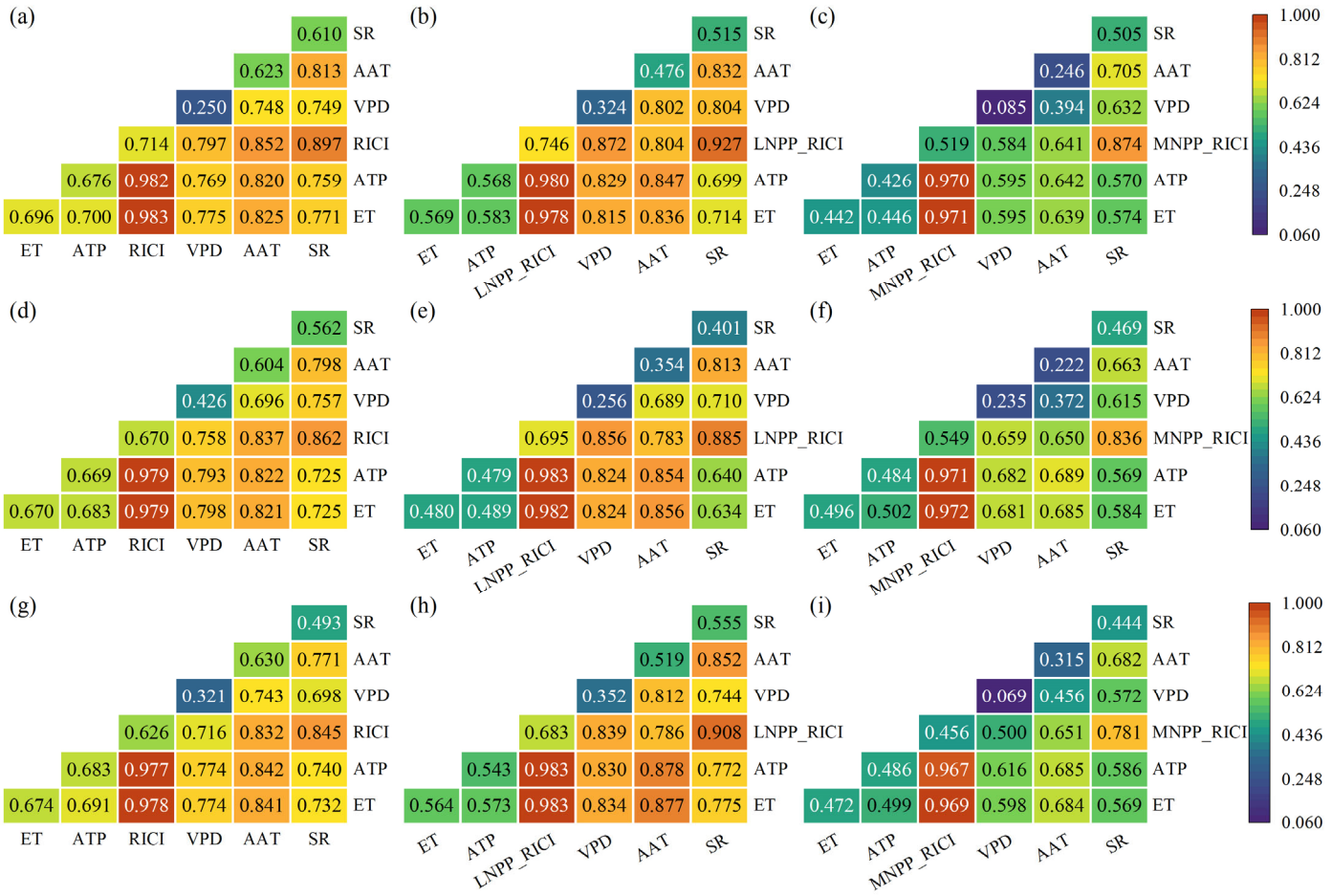

Figure 8. (**a**–**c**) are the interaction results in 2000, (**d**–**f**) are the interaction results in 2010, and (**g**–**i**) are the interaction results in 2020.

3.5.2. Prediction of NPP Under Three Development Scenarios in 2030

The prediction results show that the main LUCC is grassland and bareland, and the area of impervious surface is very small (Figure 10a–c) [78]. The dataset reveals a distinctive geographical pattern, with the north exhibiting relatively lower values, and the south, conversely, demonstrating elevated values. Furthermore, the data indicate a decline in values from east to west and an increase from west to east (Figure 10d–l). MNPP is more pronounced in the southwestern area of the Northern Tibet Plateau, and the spatial distribution of LNPP is analogous to that of MNPP (Figure 10g–l). The predicted actual values of all land use categories are largely in accordance with the theoretical values (Figure 11). The percentage of the Qinghai–Tibet Plateau that is urban is relatively low, yet it demonstrates a notable increasing trend across all three scenarios (Figure 12a–c) [78]. Furthermore, the quantity of land designated for impervious surfaces in the ED is markedly greater than that in the other two scenarios (Figure 12b), which is 36.92%. This is largely due to the influence of national strategies such as the "Western Development" initiative, which have contributed to an accelerated pace of urbanization and population growth in the region [101]. In EP, the growth rate of impervious surface land is the smallest, only 12.93%, while the growth rates of forest, waters, and wetlands are different from the other two scenarios, showing positive growth, increasing by 0.31%, 9.43%, and 20.39%, respectively (Figure 12c). This may be associated with the introduction of a number of new legislative measures in China in the past few years, focusing on the expansion of forest cultivation [102]. In comparison with the other scenarios, the expansion of bare land was curbed to some extent, with a larger reduction of −2.48% (Figure 12c), indicating that China's environmental policies had a positive effect [103]. Figure A1 illustrates a similar trend among NPP and temperature

and precipitation, exhibiting a roughly proportional relationship. While NPP exhibits an inverse relationship with radiation. Although the temperature in the CMIP6 ssp245 medium emission scenario is higher than in 2020, precipitation is much lower than in 2020, and radiation data are much higher than in 2020. These phenomena lead to a decreasing trend in climate-induced NPP in 2030. The results presented in Sections 3.3 and 3.4 indicate that climate change is the primary driver of NPP on the Tibetan Plateau. Consequently, as climate-induced NPP declines, overall NPP on the Tibetan Plateau will also decline. The ecological conservation scenario demonstrates the greatest potential for growth in forests, waters, and wetlands, with some restoration of grasslands and forests (Table 3). Despite the increase in the area of forests and other vegetation, the overall NPP on the Tibetan Plateau in 2030 is decreasing, ecological conservation only slows down the trend of decreasing NPP. Human activities have a positive effect on ecosystem improvement. For impervious surfaces, although the economic development scenario has the largest area, the corresponding total annual NPP is smaller than that of the ND (Table 3). In parallel with urban development, differentiated regulation and dynamic adjustment should be considered, and the degree of urban greening should be improved through the establishment of national parks, nature reserves, and natural parks [104].

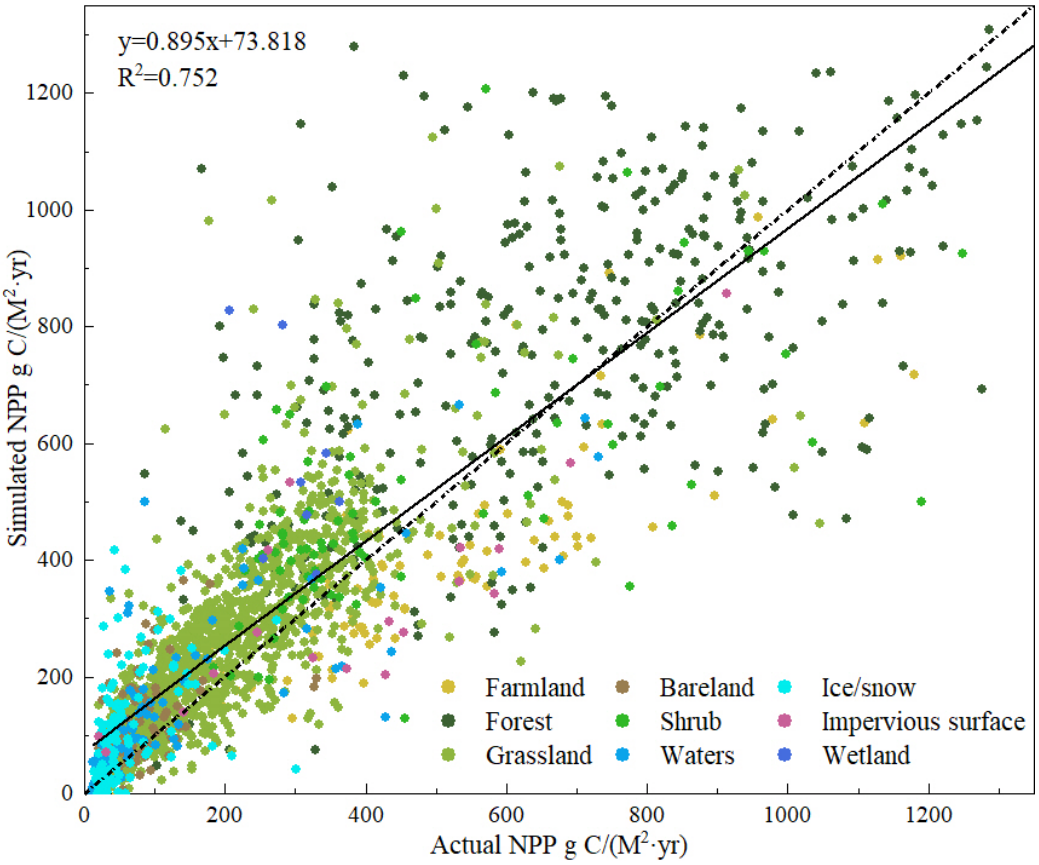

Figure 9. Comparison of simulated NPP and actual NPP.

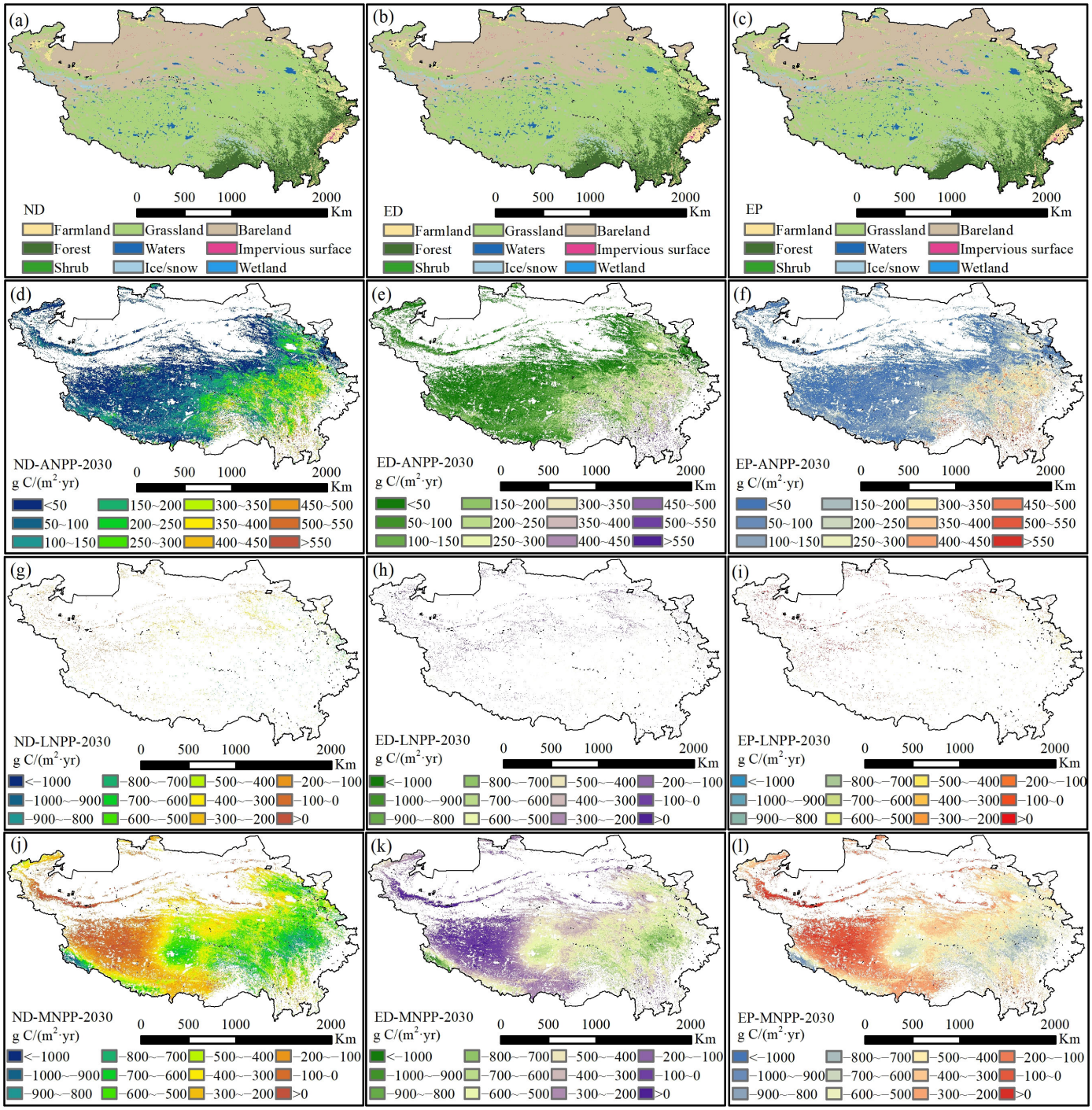

Figure 10. ND (**a**,**d**,**g**,**j**), ED (**b**,**e**,**h**,**k**), and EP (**c**,**f**,**i**,**l**) of the Qinghai–Tibet Plateau land use type, grassland ANPP, LNPP, and MNPP spatial distribution.

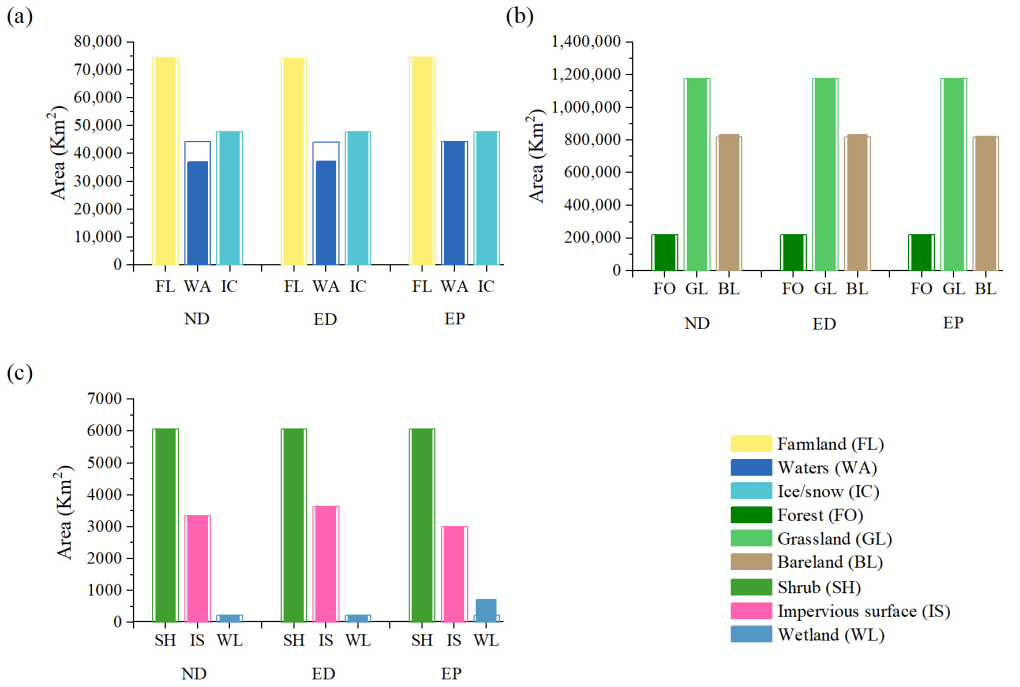

Figure 11. Different land use areas were calculated theoretically and simulated in ND, ED, and EP in 2030. The color box is the theoretical value and the color column is the actual value, (**a**) shows the theoretical and simulated values of Farmland, Waters and Ice/snow under three scenarios; (**b**) shows the theoretical and simulated values of Forest, Grassland and Bareland under three scenarios; (**c**) shows the theoretical and simulated values of Shrub, Impervious surface and Wetland under three scenarios.

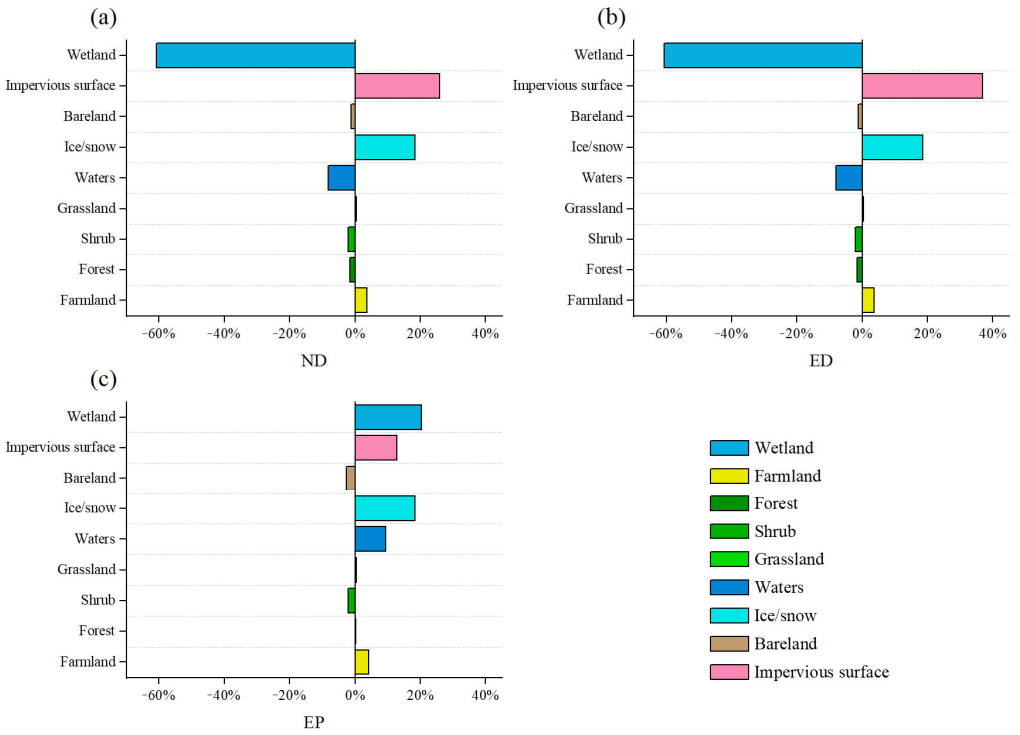

Figure 12. The alteration rates of each LUCC from 2020 to 2030 in ND, ED, and EP. (**a**) shows the alteration rates of each LUCC under the natural development scenario; (**b**) shows the alteration rates of each LUCC under the economic development scenario; (**c**) shows the alteration rates of each LUCC under the ecological protection scenario.

Table 3. NPP and growth rates by each land use type in 2030.

LUCC NPP (Gg C)	ND	Growth Rate	ED	Growth Rate	EP	Growth Rate
Farmland	13,305.2	−58.2%	13,240.0	−58.4%	12,013.8	−62.3%
Forest	157,466.8	4.3%	157,582.6	4.4%	159,362.7	5.6%
Shrub	1750.5	−42.0%	1751.1	−42.0%	1750.9	−42.0%
Grassland	146,941.6	−9.9%	146,933.7	−9.9%	146,950.6	−9.9%
Waters	1428.1	32.5%	1434.4	33.1%	1580.1	46.6%
Ice/snow	2047.5	404.7%	2039.6	402.7%	2044.4	403.9%
Bareland	14,513.4	190.0%	14,525.7	190.2%	14,279.3	185.3%
Impervious surface	425.7	−46.0%	399.8	−49.3%	399.2	−49.4%
Wetland	89.5	−13.0%	90.5	−12.1%	108.1	5.1%

4. Conclusions

The present study employed quantitative methodology to quantify the influence of LUCC on grassland NPP and to investigate how climatic change and human activity influence grassland dynamics and NPP in the Qinghai–Tibet Plateau from 2000 to 2020. The grassland area of the Qinghai–Tibet Plateau exhibited a declining trend due to land use conversion. The climatic change was the primary factor of either grassland recovery or degradation. Among the climatic factors, ET is the principal determinant of the spatial distribution of NPP. With regard to human activity factors, it was found that LNPP-RICI exerts a greater influence than MNPP-RICI. The analysis of the interaction results indicated that the interaction of climate and human activity factors enhanced their explanatory power with regard to the geographical distribution of NPP through nonlinear effects. In the future, the EP will facilitate further restoration of the vegetation on the Qinghai–Tibet Plateau and promote the growth of vegetation NPP, although urbanization will continue to progress at a slow rate. The rapid development of the city under the ED has an adverse effect on the recovery of NPP. The challenge of balancing urban development and ecological protection will be a pivotal issue. The results of this investigation may serve as a reference point for the safeguarding of grassland ecosystems, taking into consideration the multifaceted influences of human activities and climatic changes.

Author Contributions: Conceptualization, methodology, and validation, C.R. and L.H.; writing—original draft preparation, C.R.; writing—review and editing, L.H. and Z.F.; investigation, D.Z., Q.X. and G.S.; resources, L.H.; data curation, Q.X.; visualization, Q.X.; supervision, L.H. and Z.F.; project administration, T.X. All authors have read and agreed to the published version of the manuscript.

Funding: This research was supported by the Natural Science Foundation of Shandong Province, grant numbers ZR2020MD018 and ZR2020MD015; and by the National Natural Science Foundation of China, grant number 42171413.

Data Availability Statement: The original contributions presented in the study are included in the article; further inquiries can be directed to the corresponding author.

Acknowledgments: We would like to thank the kind help of the editor and the reviewers for improving the manuscript.

Conflicts of Interest: The authors declare no conflicts of interest.

Appendix A

Table A1. Statistics of grassland area and NPP associated with LUCC between 2000 and 2020 in the Qinghai–Tibet Plateau.

Change Type		Area (km^2)	Mean NPP (g C/(m^2·yr))	Total NPP (Gg C)
Unchanged grassland	Grassland to grassland	1,103,575.65	133.28	3,006,176.15
Turn out grassland	Grassland to farmland	10,781.20	274.89	35,796.78
	Grassland to forest	8162.37	456.36	41,075.05
	Grassland to bareland	45,382.40	26.37	16,933.87
	Grassland to shrub	1306.29	418.05	8099.14
	Grassland to waters	3465.61	64.97	3090.02
	Grassland to ice/snow	568.37	46.50	460.97
	Grassland to wetland	204.23	268.87	315.59
	Grassland to impervious surface	324.65	151.21	469.77
Sum	Turn out grassland	70,195.11		106,241.19
Turn in grassland	Farmland to grassland	8193.19	340.66	41,361.14
	Forest to grassland	593.42	425.49	2383.98
	Bareland to grassland	55,314.42	26.07	19,605.84
	Shrub to grassland	1699.33	379.04	9228.72
	Waters to grassland	769.23	107.23	897.32
	Ice/snow to grassland	658.44	77.67	620.39
	Wetland to grassland	162.80	315.94	1445.84
	Impervious surface to grassland	1.93	33.31	0.72
Sum	Turn in grassland	67,392.76		75,543.94

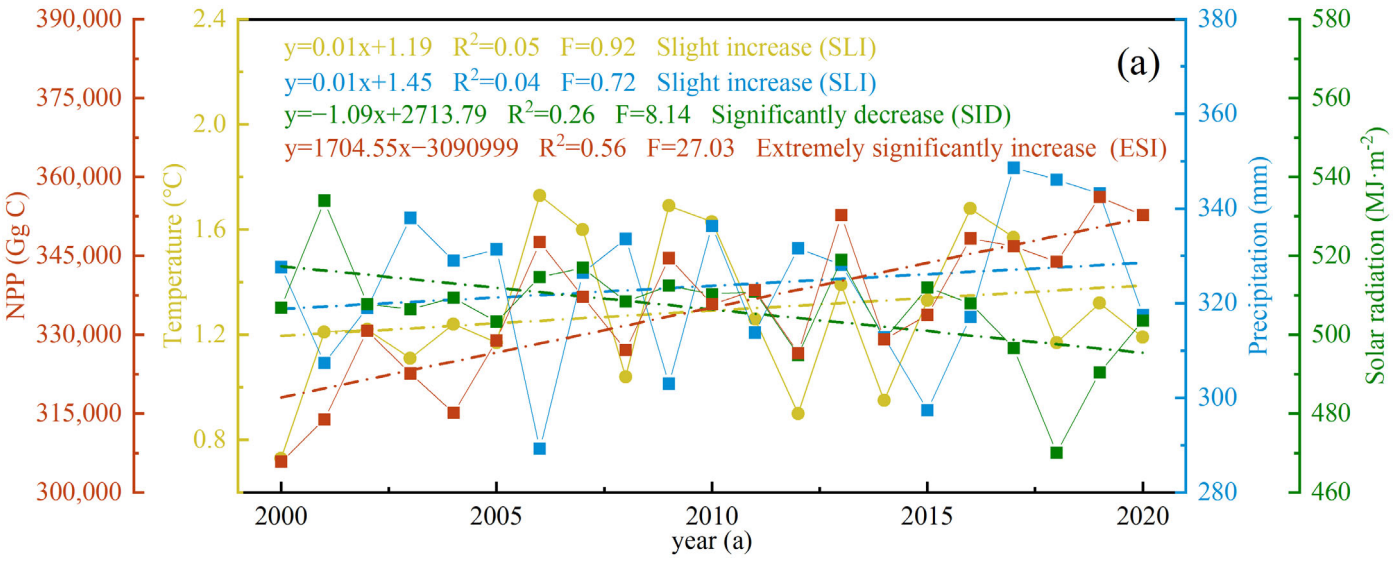

Figure A1. *Cont.*

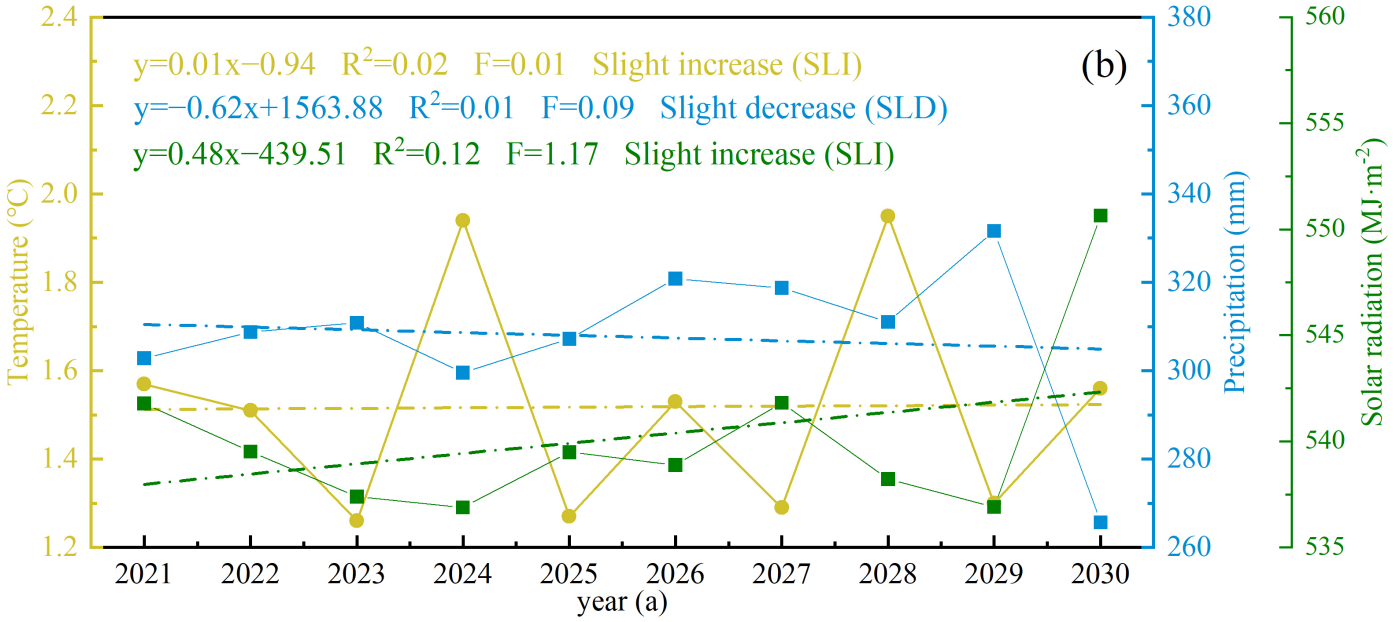

Figure A1. The temporal trends of climatic factors and NPP over the Qinghai–Tibet Plateau from 2000 to 2020 (**a**). The temporal trends of climatic factors from 2021 to 2030 (**b**).

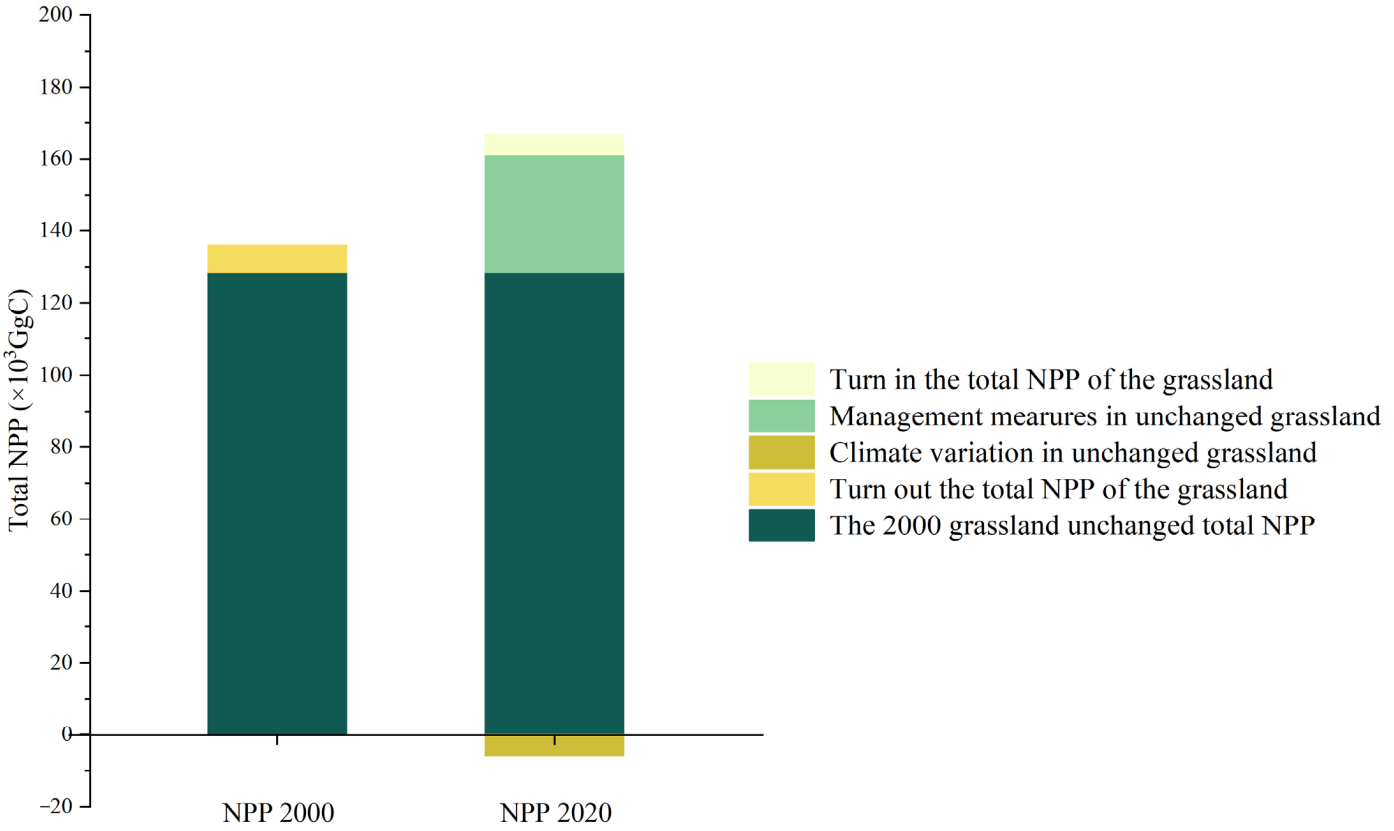

Figure A2. The total grassland NPP of Qinghai–Tibet Plateau in 2000 and 2020, and relative contributions of factors to grassland NPP change.

References

1. Squires, V.R.; Dengler, J.; Hua, L.; Feng, H. *Grasslands of the World: Diversity, Management and Conservation*; CRC Press: Boca Raton, FL, USA, 2018.
2. Wang, S.; Jia, L.; Cai, L.; Wang, Y.; Zhan, T.; Huang, A.; Fan, D. Assessment of Grassland Degradation on the Tibetan Plateau Based on Multi-Source Data. *Remote Sens.* **2022**, *14*, 6011. [CrossRef]
3. Ahlstrom, A.; Xia, J.; Arneth, A.; Luo, Y.; Smith, B. Importance of vegetation dynamics for future terrestrial carbon cycling. *Environ. Res. Lett.* **2015**, *10*, 054019. [CrossRef]
4. Taylor, P.G.; Cleveland, C.C.; Wieder, W.R.; Sullivan, B.W.; Doughty, C.E.; Dobrowski, S.Z.; Townsend, A.R. Temperature and rainfall interact to control carbon cycling in tropical forests. *Ecol. Lett.* **2017**, *20*, 779–788. [CrossRef] [PubMed]
5. Han, Y.; Lu, H.; Qiao, D. Integrated effects of meteorological factors, edaphic moisture, evapotranspiration, and leaf area index on the net primary productivity of Winter wheat− Summer maize rotation system. *Field Crops Res.* **2023**, *302*, 109080. [CrossRef]
6. Pang, Y.; Chen, C.; Guo, B.; Qi, D.; Luo, Y. Impacts of Climate Change and Anthropogenic Activities on the Net Primary Productivity of Grassland in the Southeast Tibetan Plateau. *Atmosphere* **2023**, *14*, 1217. [CrossRef]
7. Wei, X.; Yang, J.; Luo, P.; Lin, L.; Lin, K.; Guan, J. Assessment of the variation and influencing factors of vegetation NPP and carbon sink capacity under different natural conditions. *Ecol. Indic.* **2022**, *138*, 108834. [CrossRef]
8. Zheng, K.; Wei, J.; Pei, J.; Cheng, H.; Zhang, X.; Huang, F.; Li, F.; Ye, J. Impacts of climate change and human activities on grassland vegetation variation in the Chinese Loess Plateau. *Sci. Total Environ.* **2019**, *660*, 236–244. [CrossRef]
9. An, R.; Zhang, C.; Sun, M.; Wang, H.; Shen, X.; Wang, B.; Xing, F.; Huang, X.; Fan, M. Monitoring grassland degradation and restoration using a novel climate use efficiency (NCUE) index in the Tibetan Plateau, China. *Ecol. Indic.* **2021**, *131*, 108208. [CrossRef]
10. Mao, C.; Ren, Q.; He, C.; Qi, T. Assessing direct and indirect impacts of human activities on natural habitats in the Qinghai-Tibet Plateau from 2000 to 2020. *Ecol. Indic.* **2023**, *157*, 111217. [CrossRef]
11. Sun, Y.; Liu, S.; Shi, F.; An, Y.; Li, M.; Liu, Y. Spatio-temporal variations and coupling of human activity intensity and ecosystem services based on the four-quadrant model on the Qinghai-Tibet Plateau. *Sci. Total Environ.* **2020**, *743*, 140721.
12. Feng, H.; Kang, P.; Deng, Z.; Zhao, W.; Ming, H.; Zhu, X.; Wang, Z. The impact of climate change and human activities to vegetation carbon sequestration variation in Sichuan and Chongqing. *Environ. Res.* **2023**, *238*, 117138. [CrossRef] [PubMed]
13. Li, C.; de Jong, R.; Schmid, B.; Wulf, H.; Schaepman, M.E. Spatial variation of human influences on grassland biomass on the Qinghai-Tibetan plateau. *Sci. Total Environ.* **2019**, *665*, 678–689. [CrossRef] [PubMed]
14. Wang, Y.; Lv, C.; Pan, X.; Liu, Z.; Xia, P.; Zhang, C.; Liu, Z. Spatiotemporal Patterns of Light Pollution on the Tibetan Plateau over Three Decades at Multiple Scales: Implications for Conservation of Natural Habitats. *Remote Sens.* **2022**, *14*, 5755. [CrossRef]
15. Nie, Y.; Zhang, X.; Yang, Y.; Liu, Z.; He, C.; Chen, X.; Lu, T. Assessing the impacts of historical and future land-use/cover change on habitat quality in the urbanizing Lhasa River Basin on the Tibetan Plateau. *Ecol. Indic.* **2023**, *148*, 110147. [CrossRef]
16. Mao, D. *Quantitative Assessment in the Impacts of Human Activities on Net Primary Productivity of Wetlands in the Northeast China*; University of Chinese Academy of Sciences (Northeast Institute of Geography and Agroecology): Changchun, China, 2014.
17. Aizizi, Y.; Kasimu, A.; Liang, H.; Zhang, X.; Zhao, Y.; Wei, B. Evaluation of ecological space and ecological quality changes in urban agglomeration on the northern slope of the Tianshan Mountains. *Ecol. Indic.* **2023**, *146*, 109896. [CrossRef]
18. Liu, H.; Mi, Z.; Lin, L.i.; Wang, Y.; Zhang, Z.; Zhang, F.; Wang, H.; Liu, L.; Zhu, B.; Cao, G.; et al. Shifting plant species composition in response to climate change stabilizes grassland primary production. *Proc. Natl. Acad. Sci. USA* **2018**, *115*, 4051–4056. [CrossRef]
19. Dakhil, M.A.; Xiong, Q.L.; Farahatc, E.A.; Zhang, L.; Pan, K.W.; Pandey, B.; Olatunji, O.A.; Tariq, A.; Wu, X.G.; Zhang, A.P.; et al. Past and future climatic indicators for distribution pattern and conservation planning of temperate coniferous forests in southwestern China. *Ecol. Indic.* **2019**, *107*, 105559. [CrossRef]
20. Qian, D.; Fan, B.; Lan, Y.; Si, M.; Li, Q.; Guo, X. Ecosystem Service Relationships, Drivers, and Regulation Strategies in a Degraded Alpine Shrub Meadow on the Northeastern Qinghai-Tibetan Plateau. *Diversity* **2023**, *15*, 596. [CrossRef]
21. Piao, S.L.; Wang, X.H.; Ciais, P.; Zhu, B.; Wang, T.A.O.; Liu, J.I.E. Changes in satellite-derived vegetation growth trend in temperate and boreal Eurasia from 1982 to 2006. *Glob. Chang. Biol* **2011**, *17*, 3228–3239. [CrossRef]
22. Jorda-Capdevila, D.; Gampe, D.; Huber García, V.; Ludwig, R.; Sabater, S.; Vergoñós, L.; Acuña, V. Impact and mitigation of global change on freshwater-related ecosystem services in Southern Europe. *Sci. Total Environ.* **2019**, *651*, 895–908. [CrossRef]
23. Gibbs, H.K.; Salmon, J.M. Mapping the world's degraded lands. *Appl. Geogr.* **2015**, *57*, 12–21. [CrossRef]
24. Kleinherenbrink, M.; Lindenbergh, R.C.; Ditmar, P.G. Monitoring of lake level changes on the Tibetan Plateau and Tian Shan by retracking Cryosat SARIn waveforms. *J. Hydrol.* **2015**, *521*, 119–131. [CrossRef]
25. Xu, H.-J.; Wang, X.-P.; Zhang, X.-X. Alpine grasslands response to climatic factors and anthropogenic activities on the Tibetan Plateau from 2000 to 2012. *Ecol. Eng.* **2016**, *92*, 251–259. [CrossRef]
26. Gao, Y.; Zhou, X.; Wang, Q.; Wang, C.; Zhan, Z.; Chen, L.; Yan, J.; Qu, R. Vegetation net primary productivity and its response to climate change during 2001–2008 in the Tibetan Plateau. *Sci. Total Environ.* **2013**, *444*, 356–362. [CrossRef]
27. Xiong, Q.; Xiao, Y.; Halmy, M.W.A.; Dakhil, M.A.; Liang, P.; Liu, C.; Zhang, L.; Pandey, B.; Pan, K.; El Kafraway, S.B.; et al. Monitoring the impact of climate change and human activities on grassland vegetation dynamics in the northeastern Qinghai-Tibet Plateau of China during 2000–2015. *J. Arid Land* **2019**, *11*, 637–651. [CrossRef]
28. Yang, X.; Xiong, Q.; Pan, K. What is left for our next generation? Integrating ecosystem services into regional policy planning in the Three Gorges Reservoir Area of China. *Sustainability* **2019**, *11*, 3.

29. Zhao, X.; Hu, H.; Shen, H.; Zhou, D.; Zhou, L.; Myneni, R.B.; Fang, J. Satellite-indicated long-term vegetation changes and their drivers on the Mongolian Plateau. *Landsc. Ecol.* **2015**, *30*, 1599–1611. [CrossRef]
30. Xiong, Q.; Xiao, Y.; Liang, P.; Li, L.; Zhang, L.; Li, T.; Pan, K.; Liu, C. Trends in climate change and human interventions indicate grassland productivity on the Qinghai–Tibetan Plateau from 1980 to 2015. *Ecol. Indic.* **2021**, *129*, 108010. [CrossRef]
31. Zhang, J.; Wang, J.; Chen, Y.; Huang, S.; Liang, B. Spatiotemporal variation and prediction of NPP in Beijing-Tianjin-Hebei region by coupling PLUS and CASA models. *Ecol. Inform.* **2024**, *81*, 102620. [CrossRef]
32. Breidenbach, A.; Schleuss, P.-M.; Liu, S.; Schneider, D.; Dippold, M.A.; de la Haye, T.; Miehe, G.; Heitkamp, F.; Seeber, E.; Mason-Jones, K.; et al. Microbial functional changes mark irreversible course of Tibetan grassland degradation. *Nat. Commun.* **2022**, *13*, 2681. [CrossRef]
33. Wang, S.; Dai, E.; Jia, L.; Wang, Y.; Huang, A.; Liao, L.; Cai, L.; Fan, D. Assessment of multiple factors and interactions affecting grassland degradation on the Tibetan Plateau. *Ecol. Indic.* **2023**, *154*, 110509. [CrossRef]
34. Du, Y. *Prefecture-Level Adminstrative Units Boundary of Qinghai-Tibet Plateau (2015)*; National Tibetan Plateau/Third Pole Environment Data Center: Beijing, China, 2019.
35. Yao, T. Tackling on environmental changes in Tibetan Plateau with focus on water, ecosystem and adaptation. *Sci. Bull.* **2019**, *64*, 417. [CrossRef] [PubMed]
36. Yao, T.; Xue, Y.; Chen, D.; Chen, F.; Thompson, L.; Cui, P.; Koike, T.; Lau, W.K.-M.; Lettenmaier, D.; Mosbrugger, V.; et al. Recent third pole's rapid warming accompanies cryospheric melt and water cycle intensification and interactions between monsoon and environment: Multidisciplinary approach with observations, modeling, and analysis. *Bull. Am. Meteorol. Soc.* **2019**, *100*, 423–444. [CrossRef]
37. Zhang, Y.; Qi, W.; Zhou, C.; Ding, M.; Liu, L.; Gao, J.; Bai, W.; Wang, Z.; Zheng, D. Spatial and temporal variability in the net primary production of alpine grassland on the Tibetan Plateau since 1982. *J. Geogr. Sci.* **2014**, *24*, 269–287. [CrossRef]
38. Liu, Y.; Lu, C. Quantifying grass coverage trends to identify the hot plots of grassland degradation in the Tibetan Plateau during 2000–2019. *Int. J. Environ. Res. Public Health* **2021**, *18*, 416. [CrossRef]
39. Yang, J.; Huang, X. The 30 m annual land cover dataset and its dynamics in China from 1990 to 2019. *Earth Syst. Sci. Data* **2021**, *13*, 3907–3925. [CrossRef]
40. Lu, Z.; Chen, P.; Yang, Y.; Zhang, S.; Zhang, C.; Zhu, H. Exploring quantification and analyzing driving force for spatial and temporal differentiation characteristics of vegetation net primary productivity in Shandong Province, China. *Ecol. Indic.* **2023**, *153*, 110471. [CrossRef]
41. Zhang, Y.; Wang, Q.; Wang, Z.; Yang, Y.; Li, J. Impact of human activities and climate change on the grassland dynamics under different regime policies in the Mongolian Plateau. *Sci. Total Environ.* **2020**, *698*, 134304. [CrossRef]
42. Lieth, H. Modeling the primary productivity of the world. *Nat. Resour.* **1975**, *8*, 237–263.
43. Li, D.; Wang, Z. Quantitative analysis of the impact of climate change and human activities on vegetation NPP in Shaanxi Province. *Ecol. Environ. Sci.* **2022**, *31*, 1071–1079.
44. Wessels, K.J.; Prince, S.D.; Malherbe, J.; Small, J.; Frost, P.E.; VanZyl, D. Can human-induced land degradation be distinguished from the effects of rainfall variability? *A case study in South Africa. J. Arid Environ.* **2007**, *68*, 271–297.
45. Wang, J.; Zhang, T.; Fu, B. A measure of spatial stratified heterogeneity. *Ecol. Indic.* **2016**, *67*, 250–256. [CrossRef]
46. Wang, J.; Li, X.; Christakos, G.; Liao, Y.; Zhang, T.; Gu, X.; Zheng, X. Geographical Detectors-Based Health Risk Assessment and its Application in the Neural Tube Defects Study of the Heshun Region, China. *Int. J. Geogr. Inf. Sci.* **2010**, *24*, 107–127. [CrossRef]
47. Ding, H.; Hao, X. Spatiotemporal change and drivers analysis of desertification in the arid region of northwest China based on Geographic Detector. *Environ. Chall.* **2021**, *4*, 100082. [CrossRef]
48. Liang, X.; Guan, Q.; Clarke, K.C.; Liu, S.; Wang, B.; Yao, Y. Understanding the drivers of sustainable land expansion using a patch-generating land use simulation (PLUS) model: A case study in Wuhan, China. *Comput. Environ. Urban Syst.* **2021**, *85*, 101569. [CrossRef]
49. Wu, C.; Chen, B.; Huang, X.; Wei, Y.H.D. Effect of land-use change and optimization on the ecosystem service values of Jiangsu Province, China. *Ecol. Indic.* **2020**, *117*, 106507. [CrossRef]
50. Feinstein, A.R.; Cicchetti, D.V. High agreement but low kappa: I. *The problems of two paradoxes. J. Clin. Epidemiol.* **1990**, *43*, 543–549. [CrossRef]
51. Lin, W.; Sun, Y.; Nijhuis, S.; Wang, Z. Scenario-based flood risk assessment for urbanizing deltas using future land-use simulation (FLUS): Guangzhou Metropolitan Area as a case study. *Sci. Total Environ.* **2020**, *739*, 139899. [CrossRef]
52. Zhu, W.; Pan, Y.; Zhang, J. Remote sensing simulation of net primary productivity of terrestrial vegetation in China. *J. Plant Ecol.* **2007**, *31*, 413–424.
53. Ding, Z.; Zheng, H.; Li, H.; Yu, P.; Man, W.; Liu, M.; Tang, X.; Liu, Y. Afforestation-driven increases in terrestrial gross primary productivity are partly offset by urban expansion in Southwest China. *Ecol. Indic.* **2021**, *127*, 107641. [CrossRef]
54. Asefa, M.; Cao, M.; He, Y.; Mekonnen, E.; Song, X.; Yang, J. Ethiopian vegetation types, climate and topography. *Plant Divers.* **2020**, *42*, 302–311. [CrossRef] [PubMed]
55. Pfeiffer, M.; Dulamsuren, C.; Jäschke, Y.; Wesche, K. Grasslands of China and Mongolia: Spatial extent, land use and conservation. In *Grasslands of the World: Diversity, Management and Conservation*; CRC Press: Boca Raton, FL, USA, 2018; pp. 170–198.
56. Wang, Y.; Zhou, L.; Yang, G.; Guo, R.; Xia, C.; Liu, Y. Performance and obstacle tracking to natural forest resource protection project: A rangers' case of Qilian mountain, China. *Int. J. Environ. Res. Public Health* **2020**, *17*, 5672. [CrossRef]

57. Li, Z.; Sun, X.; Huang, Z.; Zhang, X.; Wang, Z.; Li, S.; Zheng, W.; Zhai, B. Changes in nutrient balance, environmental efects, and green development afer returning farmland to forests: A case study in Ningxia, China. *Sci. Total Environ.* **2020**, *735*, 139370. [CrossRef]
58. Duan, Q.; Luo, L.; Zhao, W.; Zhuang, Y.; Liu, F. Mapping and evaluating human pressure changes in the Qilian mountains. *Remote Sens.* **2021**, *13*, 2400. [CrossRef]
59. Harris, R.B.; Samberg, L.H.; Yeh, E.T.; Smith, A.T.; Wenying, W.; Junbang, W. Rangeland responses to pastoralists' grazing management on a Tibetan steppe grassland, Qinghai Province, China. *Rangel. J.* **2016**, *38*, 1–15. [CrossRef]
60. Yang, L.; Zhao, G.; Mu, X.; Lan, Z.; Jiao, J.; An, S.; Wu, Y.; Miping, P. Integrated assessments of land degradation on the Qinghai-Tibet plateau. *Ecol. Indic.* **2023**, *147*, 109945. [CrossRef]
61. Yang, J.; Xie, B.; Zhang, D. Spatial–temporal evolution of ESV and its response to land use change in the Yellow River Basin, China. *Sci. Rep.* **2022**, *12*, 13103. [CrossRef]
62. Xu, R.; Shi, P.; Gao, M.; Wang, Y.; Wang, G.; Su, B.; Huang, J.; Lin, Q.; Jiang, T. Projected land use changes in the Qinghai-Tibet Plateau at the carbon peak and carbon neutrality targets. *Sci. China Earth Sci.* **2023**, *66*, 1383–1398. [CrossRef]
63. Hao, J.; Zhi, L.; Li, X.; Dong, S.; Li, W. Temporal and spatial evolution characteristics and relationships of land use pattern and ecosystem services in Qinghai-Tibet Plateau, China. *Chin. J. Appl. Ecol.* **2023**, *34*, 11.
64. Wang, X.; Piao, S.; Ciais, P.; Friedlingstein, P.; Myneni, R.B.; Cox, P.; Heimann, M.; Miller, J.; Peng, S.; Wang, T.; et al. A two-fold increase of carbon cycle sensitivity to tropical temperature variations. *Nature* **2014**, *506*, 212–215. [CrossRef]
65. Sha, Z.; Xie, Y.; Tan, X.; Bai, Y.; Li, J.; Liu, X. Assessing the impacts of human activities and climate variations on grassland productivity by partial least squares structural equation modeling (PLS-SEM). *J. Arid Land* **2017**, *9*, 473–488. [CrossRef]
66. Chen, T.; Tang, G.; Yuan, Y.; Guo, H.; Xu, Z.; Jiang, G.; Chen, X. Unraveling the relative impacts of climate change and human activities on grassland productivity in Central Asia over last three decades. *Sci. Total Environ.* **2020**, *743*, 140649. [CrossRef] [PubMed]
67. Yu, H.; Ding, Q.; Meng, B.; Lv, Y.; Liu, C.; Zhang, X.; Sun, Y.; Li, M.; Yi, S. The relative contributions of climate and grazing on the dynamics of grassland NPP and PUE on the qinghai-Tibet plateau. *Remote Sens.* **2021**, *13*, 3424. [CrossRef]
68. Guo, J.; Zhai, L.; Sang, H.; Cheng, S.; Li, H. Effects of hydrothermal factors and human activities on the vegetation coverage of the Qinghai-Tibet Plateau. *Sci. Rep.* **2023**, *13*, 12488. [CrossRef] [PubMed]
69. Zhang, J.; Zhang, Y.; Qin, Y.; Lu, X.; Cao, J. The spatiotemporal pattern of grassland NPP in Inner Mongolia was more sensitive to moisture and human activities than that in the Qinghai-Tibetan Plateau. *Glob. Ecol. Conserv.* **2023**, *48*, e02709. [CrossRef]
70. Di Pasquale, G.; Saracino, A.; Bosso, L.; Russo, D.; Moroni, A.; Bonanomi, G.; Allevato, E. Coastal Pine-Oak Glacial Refugia in the Mediterranean Basin: A Biogeographic Approach Based on Charcoal Analysis and Spatial Modelling. *Forests* **2020**, *11*, 673. [CrossRef]
71. Huang, K.; Zhang, Y.; Zhu, J.; Liu, Y.; Zu, J.; Zhang, J. The influences of climate change and human activities on vegetation dynamics in the Qinghai-Tibet Plateau. *Remote Sens.* **2016**, *8*, 876. [CrossRef]
72. Luo, L.; Ma, W.; Zhuang, Y.; Zhang, Y.; Yi, S.; Xu, J.; Long, Y.; Ma, D.; Zhang, Z. The impacts of climate change and human activities on alpine vegetation and permafrost in the Qinghai-Tibet Engineering Corridor. *Ecol. Indic.* **2018**, *93*, 24–25. [CrossRef]
73. Zhou, Y.; Zhang, L.; Fensholt, R.; Wang, K.; Vitkovskaya, I.; Tian, F. Climate contributions to vegetation variations in central Asian Drylands: Pre-and post-USSR collapse. *Remote Sens.* **2015**, *7*, 2449–2470. [CrossRef]
74. Gang, C.; Zhou, W.; Chen, Y.; Wang, Z.; Sun, Z.; Li, J.; Qi, J.; Odeh, Q. Quantitative assessment of the contributions of climate change and human activities on global grassland degradation. *Environ. Earth Sci.* **2014**, *72*, 4273–4282. [CrossRef]
75. Mowll, W.; Blumenthal, D.M.; Cherwin, K.; Smith, A.; Symstad, A.J.; Vermeire, L.T.; Collins, S.L.; Smith, M.D.; Knapp, A.K. Climatic controls of aboveground net primary production in semi-arid grasslands along a latitudinal gradient portend low sensitivity to warming. *Oecologia* **2015**, *177*, 959–969. [CrossRef] [PubMed]
76. Li, C.; Li, X.; Luo, D.; He, Y.; Chen, F.; Zhang, B.; Qin, Q. Spatiotemporal pattern of vegetation ecology quality and its response to climate change between 2000–2017 in China. *Sustainability* **2021**, *13*, 1419. [CrossRef]
77. Malek, Ž.; Verburg, P.H.; Geijzendorffer, I.R.; Bondeau, A.; Cramer, W. Global change effects on land management in the Mediterranean region. *Glob. Environ. Chang.* **2018**, *50*, 238–254. [CrossRef]
78. Jin, X.; Jiang, P.; Ma, D.; Li, M. Land system evolution of Qinghai-Tibetan Plateau under various development strategies. *Appl. Geogr.* **2019**, *104*, 1–9. [CrossRef]
79. Pan, Y.; Wu, J.; Zhang, Y.; Zhang, X.; Yu, C. Simultaneous enhancement of ecosystem services and poverty reduction through adjustments to subsidy policies relating to grassland use in Tibet, China. *Ecosyst. Serv.* **2021**, *48*, 101254. [CrossRef]
80. Song, C.; Huang, B.; Richards, K.; Ke, L.; Hien Phan, V. Accelerated lake expansion on the Tibetan Plateau in the 2000s: Induced by glacial melting or other processes? *Water Resour. Res.* **2014**, *50*, 3170–3186. [CrossRef]
81. Wang, Y.; Wang, J.; Li, S.; Qin, D. Vulnerability of the Tibetan Pastoral Systems to Climate and Global Change. *Ecol. Soc.* **2014**, *19*, 8. [CrossRef]
82. Yan, Z.; Wu, N.; Yeshi, D.; Ru, J. A review of rangeland privatization and its implications in the Tibetan Plateau, China. *Nomadic Peoples* **2005**, *9*, 31–51.
83. Furqat, T.; Sanjar, B. The role of nomadic peoples in the development of ustrushona urban development. *Asian J. Multidimens. Res.* **2020**, *9*, 140–145. [CrossRef]

84. Kumar, N.; Dogra, P.K.; Kumari, V.S.A.; Thakur, A. *Enhancing Profitability of Nomadic Gaddi Goat Production System for Augmenting Farmer's Income*; The Indian Society of Animal Production and Management: Ludhiana, Indian, 2020.
85. Anees, M.M.; Mann, D.; Sharma, M.; Banzhaf, E.; Joshi, P.K. Assessment of Urban Dynamics to Understand Spatiotemporal Differentiation at Various Scales Using Remote Sensing and Geospatial Tools. *Remote Sens.* **2020**, *12*, 1306. [CrossRef]
86. Zhao, Z.; Liu, J.; Shao, Q. Characteristic analysis of land cover change in nature reserve of Three River's Source Regions. *Sci. Geogr. Sin.* **2010**, *30*, 415–420.
87. Xue, H.; Chen, Y.; Dong, G.; Li, J. Quantitative analysis of spatiotemporal changes and driving forces of vegetation net primary productivity (NPP) in the Qimeng region of Inner Mongolia. *Ecol. Indic.* **2023**, *154*, 110610. [CrossRef]
88. Yang, D.; Wang, F. *The Application and Research of Mathematical Model in Ecology 30*; China Ocean Press: Beijing, China, 2015; Volume 211.
89. Potter, C.; Klooster, S.; Genovese, V. Net primary production of terrestrial ecosystems from 2000 to 2009. *Clim. Chang.* **2012**, *115*, 365–378. [CrossRef]
90. Alkama, R.; Forzieri, G.; Duveiller, G.; Grassi, G.; Liang, S.; Cescatti, A. Vegetation-based climate mitigation in a warmer and greener World. *Nat. Commun.* **2022**, *13*, 606. [CrossRef]
91. Wu, X.; Zhang, R.; Bento, V.A.; Leng, S.; Qi, J.; Zeng, J.; Wang, Q. The effect of drought on vegetation gross primary productivity under different vegetation types across China from 2001 to 2020. *Remote Sens.* **2022**, *14*, 4658. [CrossRef]
92. Zheng, H.; Miao, C.; Li, X.; Kong, D.; Gou, J.; Wu, J.; Zhang, S. Effects of vegetation changes and multiple environmental factors on evapotranspiration across China over the past 34 years. *Earth's Future* **2022**, *10*, e2021EF002564. [CrossRef]
93. Yan, H.; Zhan, J.; Jiang, Q.O.; Yuan, Y.; Li, Z. Multilevel modeling of NPP change and impacts of water resources in the Lower Heihe River Basin. *Phys. Chem. Earth* **2015**, *79*, 29–39. [CrossRef]
94. Alijani, Z.; Hosseinali, F.; Biswas, A. Spatio-temporal evolution of agricultural land use change drivers: A case study from Chalous region, Iran. *J. Environ. Manag.* **2020**, *262*, 110326. [CrossRef]
95. Foley, J.A.; DeFries, R.; Asner, G.P.; Barford, C.; Bonan, G.; Carpenter, S.R.; Chapin, F.S.; Coe, M.T.; Daily, G.C.; Gibbs, H.K. Global consequences of land use. *Science* **2005**, *309*, 570–574. [CrossRef]
96. Zhang, X.; Lu, X.; Wang, X. Spatial-temporal NDVI variation of different alpine grassland classes and groups in Northern Tibet from 2000 to 2013. *Mt. Res. Dev.* **2015**, *35*, 254–263. [CrossRef]
97. Rahman, M.N.; Azim, S.A.; Jannat, F.A.; Rony, M.R.H.; Ahmad, B.; Sarkar, M.A.R. Quantification of rainfall, temperature, and reference evapotranspiration trend and their interrelationship in sub-climatic zones of Bangladesh. *Heliyon* **2023**, *9*, e19559. [CrossRef] [PubMed]
98. Li, C.; Hao, J.; Zhang, G.; Fang, H.; Wang, Y.; Lu, H. Runoff variations affected by climate change and human activities in Yarlung Zangbo River, southeastern Tibetan Plateau. *Catena* **2023**, *230*, 107184. [CrossRef]
99. Li, H.; He, Y.; Zhang, L.; Cao, S.; Sun, Q. Spatiotemporal changes of Gross Primary Production in the Yellow River Basin of China under the influence of climate-driven and human-activity. *Glob. Ecol. Conserv.* **2023**, *46*, e02550. [CrossRef]
100. Wang, G.; Peng, W.; Zhang, L.; Zhang, J. Quantifying the impacts of natural and human factors on changes in NPP using an optimal parameters-based geographical detector. *Ecol. Indic.* **2023**, *155*, 111018. [CrossRef]
101. Fang, C.; Li, G.; Bao, C.; Wang, Z.; Qi, W.; Ma, H.; Sun, S.; Fan, Y.; Chen, W. How many people can the Qinghai-Tibet Plateau hold, and how large cities can be built in recent hundred years? *Sci. Total Environ.* **2024**, *927*, 172404. [CrossRef]
102. Cao, S.; Chen, L.; Shankman, D.; Wang, C.; Wang, X.; Zhang, H. Excessive reliance on afforestation in China's arid and semi-arid regions: Lessons in ecological restoration. *Earth-Sci. Rev.* **2011**, *104*, 240–245. [CrossRef]
103. Feng, X.; Li, Y.; Li, P.; Ding, Y.; Wang, Y. Study on the regulatory behaviors of grazing households to maintain grassland–livestock balance under the Grassland Ecological Compensation Policy. *Chin. J. Grassl.* **2019**, *41*, 132–142.
104. Zhou, Y.; Zhang, X.; Yu, H.; Liu, Q.; Xu, L. Land use-driven changes in ecosystem service values and simulation of future scenarios: A case study of the Qinghai–Tibet Plateau. *Sustainability* **2021**, *13*, 4079. [CrossRef]

Disclaimer/Publisher's Note: The statements, opinions and data contained in all publications are solely those of the individual author(s) and contributor(s) and not of MDPI and/or the editor(s). MDPI and/or the editor(s) disclaim responsibility for any injury to people or property resulting from any ideas, methods, instructions or products referred to in the content.